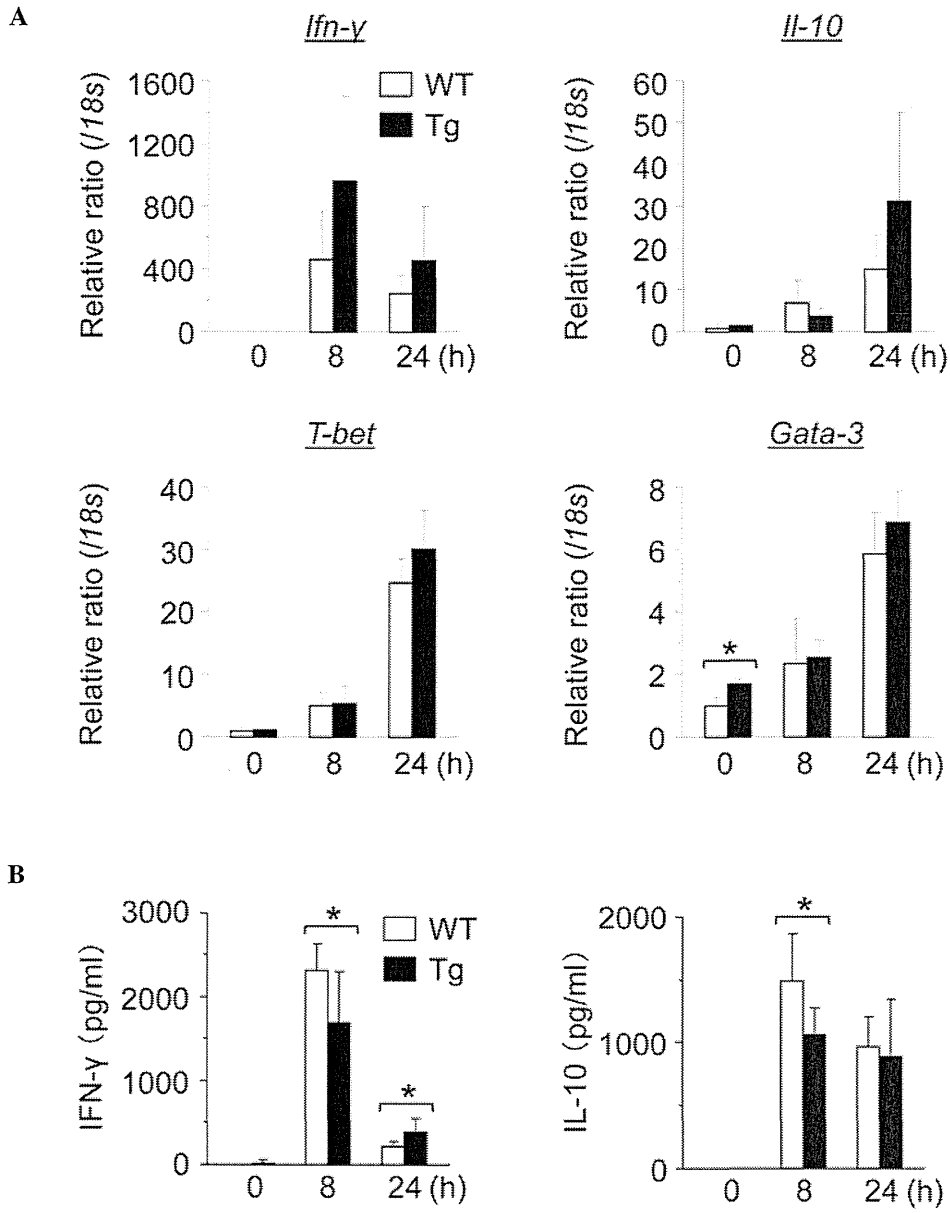

Figure 2. Expression of *in vivo*-activated cytokines demonstrates no significant changes. Hepatic gene expression in WT and GnT-V Tg mice 0, 8, or 24 h after the injection of ConA at 12.5 mg/kg BW. Gene expression of (A) *Ifn-γ, Il-10, T-bet* and *Gata-3* in mouse livers was evaluated using reverse transcription quantitative polymerase chain reaction. The mRNA expression levels were normalized relative to the mRNA expression of *18s* and are expressed in arbitrary units. The results are expressed as the mean ± standard deviation; *P<0.05. (B) Serum cytokine levels in the WT and GnT-V Tg mice 0, 8, or 24 h after the injection of ConA at 12.5 mg/kg BW. Serum levels of IFN-γ and IL-10 were measured by ELISA at the indicated time points. Results are expressed as the mean ± standard deviation; *P<0.05. GnT-V, *N*-acetylglucosaminyltransferase V; WT, wild-type; Tg, transgenic; ConA, concanavalin A; BW, body weight; Ifn, interferon; IL, interleukin.

levels of IFN-γ and IL-10 in the GnT-V Tg mice 8 h after the injection of ConA were significantly lower compared with those in the WT mice (Fig. 2B).

Th1 to Th2 cytokine shift in GnT-V Tg mouse splenic lymphocytes in vitro. T cells are important in ConA-induced hepatitis (1,4,5). To investigate function of splenic lymphocytes from the WT and GnT-V Tg mice in cytokine production, the mouse splenic lymphocytes were stimulated with anti-CD3/CD28 antibodies *in vitro*. Levels of the IFN-γ Th1 cytokine were significantly lower in the GnT-V Tg compared with the WT mouse splenic lymphocytes (Fig. 3A), whereas levels of the IL-10 Th2 cytokine were higher in the GnT-V Tg mouse splenic lymphocytes compared with the WT lymphocytes.

ConA activates lymphocyte function, including cytokine production (1,4,5). Subsequently, mouse splenic lymphocytes were stimulated with ConA *in vitro*. As was observed following stimulation with the anti-CD3/CD28 antibodies, the levels of gene expression and the production of IFN-γ in the GnT-V Tg mouse splenic lymphocytes were lower compared with those in the WT, whereas the levels of IL-10 were higher (Fig. 3B and C). IFN-γ is considered a typical pro-inflammatory cytokine (10,11) and IL-10 is known to protect the liver from ConA-induced hepatitis (14,15). Therefore, the exacerbated ConA-induced

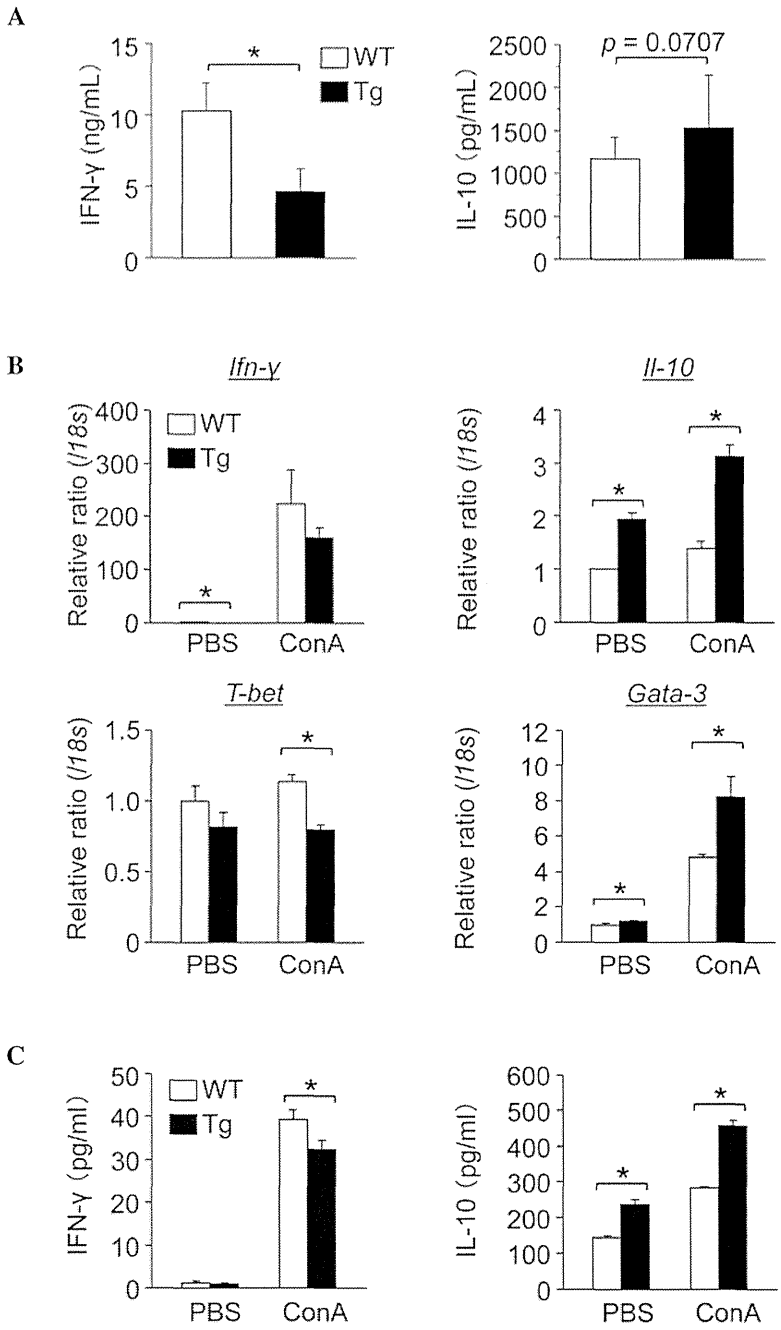

Figure 3. GnT-V Tg mouse splenic lymphocytes produce increased Th2 cytokines. (A) Anti-CD3/CD28 antibody-induced cytokine production levels secreted into the medium from splenic lymphocytes. Mononuclear cells of the spleen, isolated from WT and GnT-V Tg mice, were cultured for 48 h in the presence of anti-CD3 (5 μg/ml) and anti-CD28 (5 μg/ml) antibodies and levels of IFN-γ and IL-10 were measured using ELISA. The results are expressed as the mean ± standard deviation (n=3-8); *P<0.05. (B) Gene expression of cytokinines in the splenic lymphocytes following ConA stimulation is shown. Splenic lymphocytes from WT and GnT-V Tg mice were cultured for 24 h in the presence of ConA (5 μg/ml) and the gene expression levels of *Ifn-γ, Il-10, T-bet* and *Gata-3* were measured by reverse transcription quantitative polymerase chain reaction. The mRNA expression levels were normalized relative to that of *18s* and are expressed in arbitrary units. The results are expressed as the mean ± standard deviation (n=3); *P<0.05. (C) ConA-induced cytokine production levels secreted into the medium from splenic lymphocytes. Splenic lymphocytes from WT and GnT-V Tg mice were cultured for 24 h in the presence of ConA (5 μg/ml) and levels of IFN-γ and IL-10 were measured using ELISA. Results are expressed as the mean ± standard deviation (n=3); *P<0.05. WT, wild-type mouse splenic lymphocytes; GnT-V, *N*-acetylglucosaminyltransferase V; Tg, GnT-V transgenic mouse splenic lymphocytes; ConA, concanavalin A; BW, body weight; Ifn, interferon; IL, interleukin; PBS, phosphate-buffered saline; Th, T helper; CD, cluster of differentiation.

hepatitis in the GnT-V Tg mice *in vivo* was not explained by these *in vitro* results.

No difference is observed in the binding affinity of ConA to LSECs between WT and GnT-V Tg mice. The binding of ConA to the mannose gland of the LSEC surface, which is followed by LSEC damage, recruits T lymphocytes from the sinusoidal circulation and is an early event in T cell-mediated liver injury (5). The subsequent loss of function of the LSEC barrier exposes the underlying hepatocytes to further attack from activated T lymphocytes (5-7). To examine the binding affinity of ConA to LSECs from the WT and the GnT-V Tg mice, ConA lectin blotting and flow cytometric analysis were performed. The purity of the isolated LSECs was >75% (Fig. 4A).

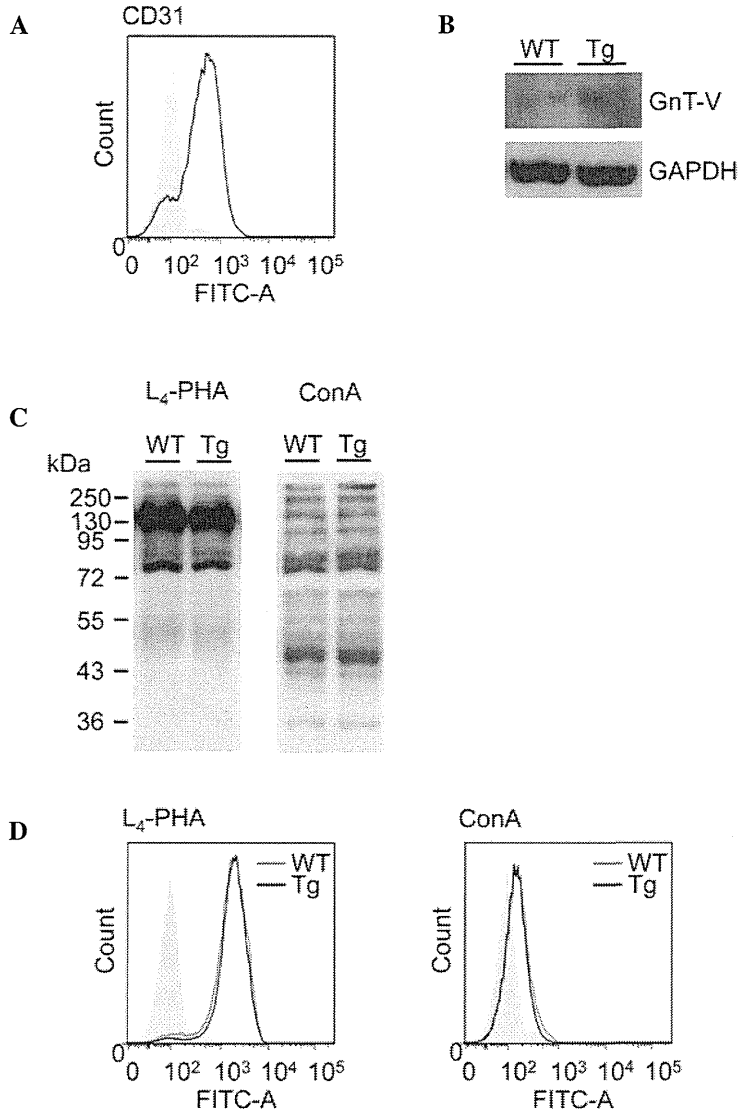

Figure 4. Binding affinity of ConA to LSECs does not differ between WT and GnT-V Tg mice. (A) Purity of the LSECs was analyzed by the expression of the cell surface marker, CD31. (B) Expression of GnT-V in LSECs was characterized by immunoblotting against GnT-V. Immunoblotting against GAPDH was performed as a loading control. (C) β1-6 *N*-acetylglucosamine branching (the product of GnT-V) and the binding affinity of ConA to LSECs were assessed by L_4-PHA and ConA by lectin blot analysis. (D) Results of the L_4-PHA and ConA lectin flow cytometric analysis. Data are representative of experiments repeated more than three times using three mice per experiment. WT, wild-type mouse LSECs; GnT-V, *N*-acetylglucosaminyltransferase V; Tg, GnT-V transgenic mouse LSECs; ConA, concanavalin A; LSEC, liver sinusoidal endothelial cell; CD, cluster of differentiation; L_4-PHA, leukoagglutinating phytohemagglutinin; FITC, fluorescein isothiocyanate.

To investigate the difference in the GnT-V and β1-6 GlcNAc branching of *N*-glycans expression in LSECs from the WT and GnT-V Tg mice, GnT-V immunoblotting, L_4-PHA lectin blotting and flow cytometric analysis were performed (Fig. 4B-D). L_4-PHA binds to the β1-6 GlcNAc branching of *N*-glycans, which is the product of GnT-V. Although the protein expression of GnT-V was increased in the GnT-V Tg mouse LSECs compared with the WT mouse LSECs (Fig. 4B), the expression of β1-6 GlcNAc branching of *N*-glycans, determined by L_4-PHA lectin blotting and flow cytometric analysis, did not differ between the WT and GnT-V Tg mouse LSECs (Fig. 4C, left panel and 4D, left panel). ConA lectin blotting and flow cytometric analysis also revealed no difference in the binding affinity of ConA to the LSECs between the WT and GnT-V Tg mouse LSECs (Fig. 4Cand D).

Number of hepatic macrophages is significantly increased in GnT-V Tg compared with WT mice. Subsequently, the hepatic immune cells were examined and the liver MNC subset was investigated prior to or following the injection of ConA. Notably, the number of CD11b-positive cells was significantly increased in the GnT-V Tg liver compared with the WT mouse liver prior to and 2 h after ConA injection (Fig. 5A and B). In addition, the gene expression of the macrophage markers F4/80 and CD68 were significantly increased in the Tg mouse MNCs (Fig. 5C). F4/80 immunohistochemical staining of the livers also revealed that the number of hepatic F4/80-positive macrophages was significantly increased in the GnT-V Tg mice compared with the WT mice (Fig. 6A and B). These results indicated that the number of hepatic macrophages was higher in the GnT-V Tg mice than in the WT mice.

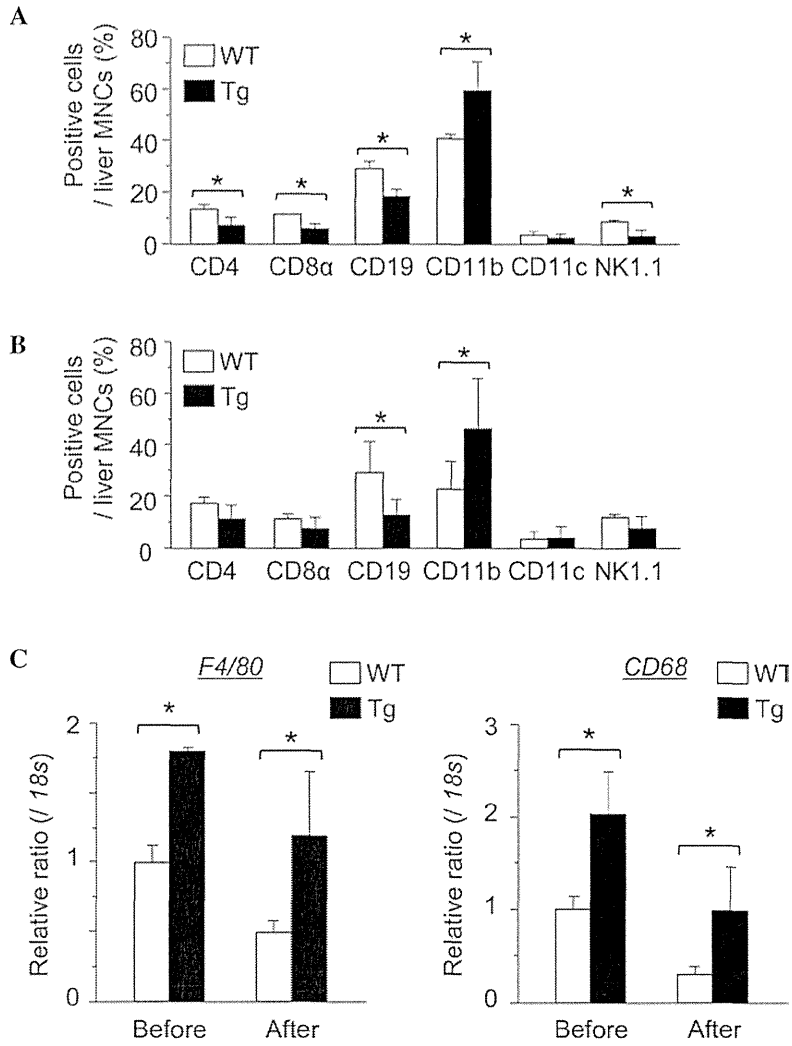

Figure 5. Hepatic macrophages are significantly increased in GnT-V Tg, vs. WT mice. Subset analyses of liver MNCs in the WT and GnT-V Tg mice (A) prior to and (B) 2 h after the injection of ConA at 12.5 mg/kg body weight were performed by flow cytometry. (C) Gene expression levels of the macrophage markers, F4/80 and CD68, in the MNCs before and 2 h after injection of ConA is shown. Results are expressed as the mean ± standard deviation (n=3); *P<0.05. WT, wild-type mouse liver MNCs; MNCs; ConA, concanavalin A; CD, cluster of differentiation; GnT-V, *N*-acetylglucosaminyltransferase V; Tg GnT-V, transgenic mouse liver; MNC, mononuclear cells.

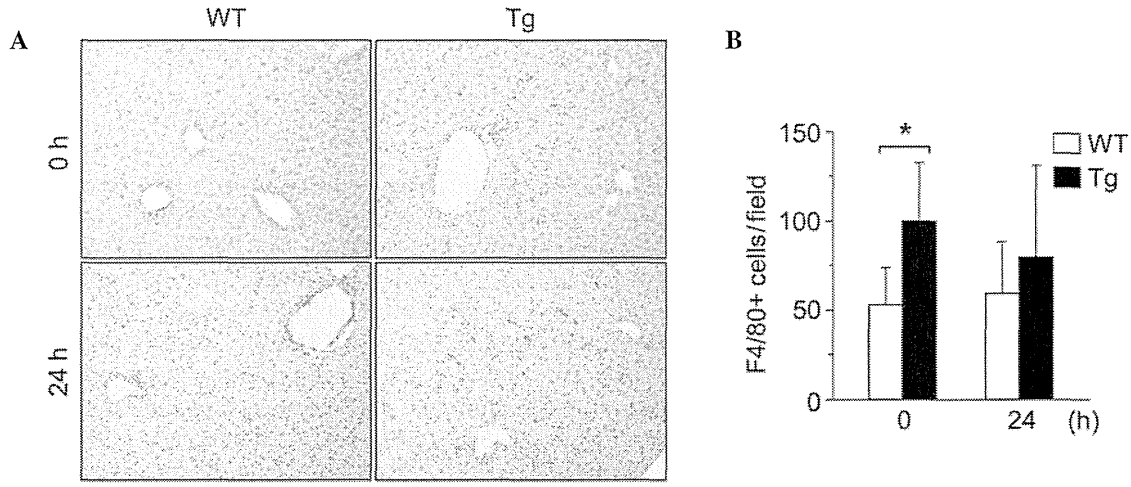

Figure 6. Number of hepatic F4/80-positive macrophages in GnT-V Tg mice is significantly increased compared with the number in WT mice. (A) Photomicrographs show representative mouse livers stained with anti-F4/80 antibody prior to (0 h) and 24 h after the injection of ConA at 12.5 mg/kg body weight (magnification, x200). (B) Quantification of the number of F4/80 positive cells/field is shown. Results are expressed as the mean ± standard deviation (0 h, n=9; 24 h, n=18); *P<0.05, compared with WT. WT, wild-type mouse liver; GnT-V, *N*-acetylglucosaminyltransferase V; Tg, GnT-V transgenic mouse liver; ConA, concanavalin A.

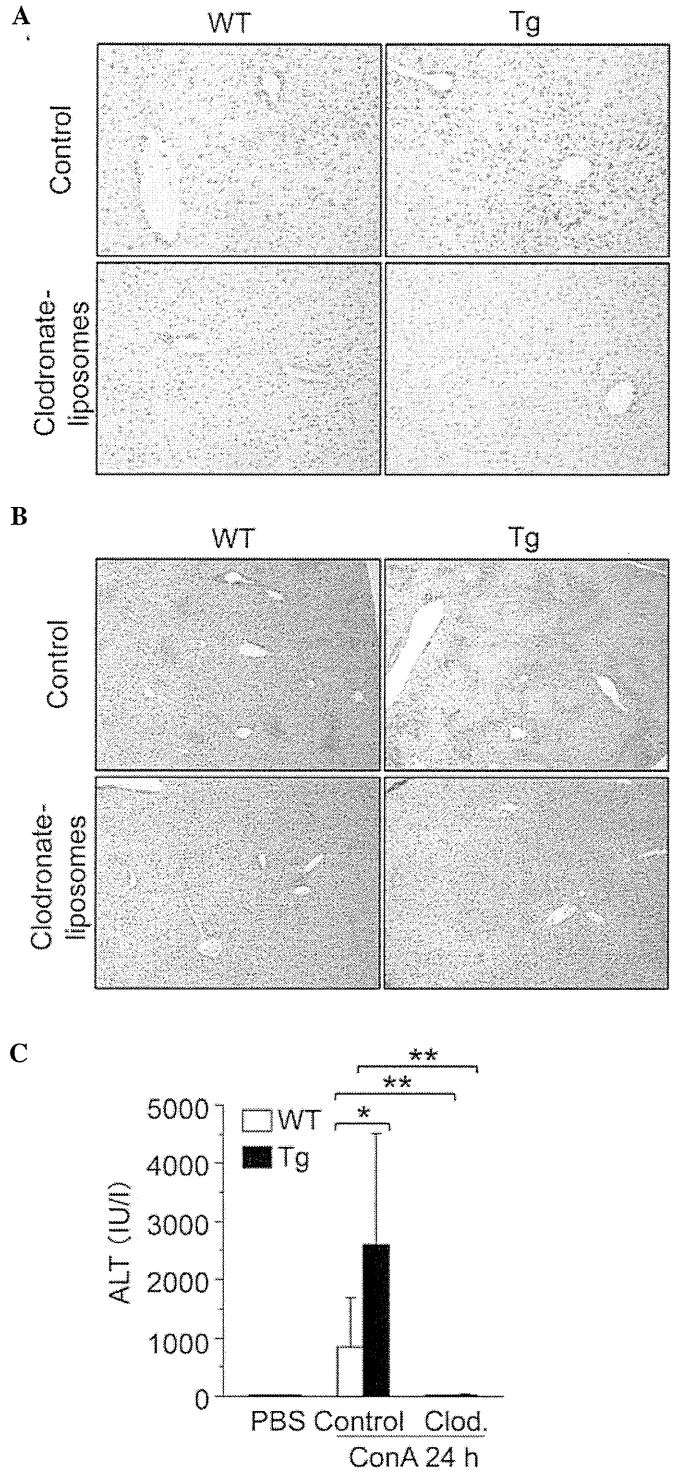

Figure 7. Hepatic macrophage depletion reduces the difference in the degree of hepatitis between WT and GnT-V Tg mice. (A) Representative photomicrographs mouse livers stained with anti-F4/80 antibody 24 h after the injection of ConA at 12.5 mg/kg BW (magnification, x200). Clodronate-liposomes were injected 2 days prior to ConA administration. (B) Representative photomicrographs of hematoxylin and eosin stained mouse livers 24 h after the injection of ConA at 12.5 mg/kg BW (magnification, x40). (C) Levels of serum ALT in mice (n=6) 24 h after the injection of ConA at 12.5 mg/kg BW. Results are expressed as the mean ± standard deviation; $^{*}P<0.05$ and $^{**}P<0.01$. WT, wild-type mice; GnT-V, *N*-acetylglucosaminyltransferase V; Tg, GnT-V transegenic mice; Clod, clodronate-liposomes; ALT, alanine aminotransferase; PBS, phosphate-buffered saline; ConA, concanavalin A; BW, body weight.

Depletion of hepatic macrophages reduces the degree of difference in ConA-induced hepatitis between WT and GnT-V Tg mice. To investigate the effect of hepatic macrophages in ConA-induced hepatitis in GnT-V Tg mice, macrophages were depleted from the WT and GnT-V Tg mice using clodronate-liposomes, and the severity of ConA-induced hepatitis was determined. The depletion of hepatic macrophages was confirmed by immunohistochemical staining with anti-F4/80 antibody (Fig. 7A). Macrophage depletion significantly suppressed ConA-induced liver injury in the WT and GnT-V Tg mice and it reduced the differences in liver injury between the WT and GnT-V Tg mice (Fig. 7B and C).

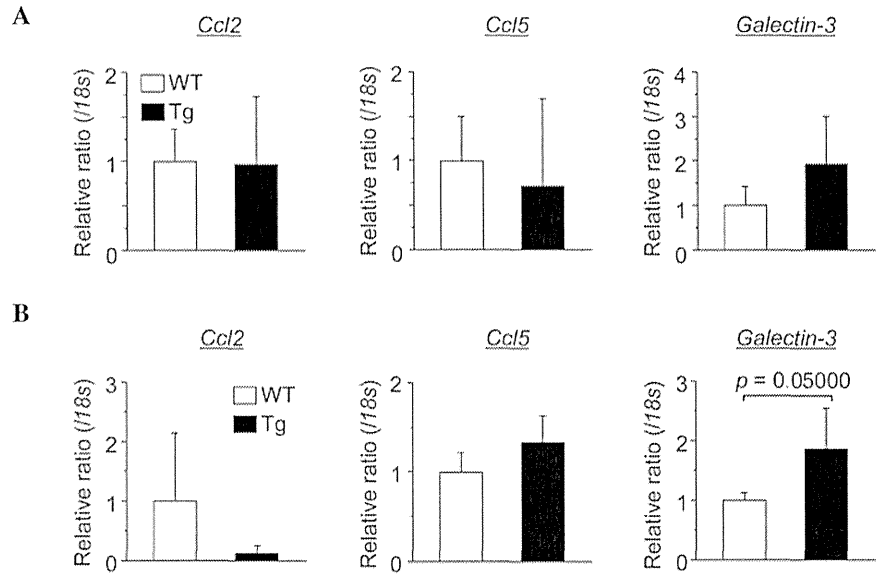

Figure 8. Gene expression of galectin-3 is elevated in Tg mouse hepatocytes. (A) Gene expression levels of macrophage chemoattractants in the mouse liver. (B) Gene expression levels of macrophage chemoattractants in the mouse hepatocytes. Results are expressed as the mean ± standard deviation. WT, wild-type mice; GnT-V, *N*-acetylglucosaminyltransferase V; Tg, GnT-V transgenic mice; Ccl, C-C chemokine ligand.

Expression of galectin-3 is elevated in Tg mouse hepatocytes. To elucidate the reason why the number of liver macrophages in the Tg mice was elevated compared with the number in the WT mice, the expression of macrophage chemoattractant genes (*Ccl2, Ccl5* and *Galectin-3*) were investigated in mouse hepatocytes (Fig. 8). The results demomnstrated that the gene expression of *galectin-3* was elevated in the Tg mouse hepatocytes compared with the WT mouse hepatocytes.

Discussion

In the present study, it was initially observed that ectopic expression of GnT-V exacerbated ConA-induced hepatitis despite the Th1 to Th2 cytokine shift observed in the GnT-V Tg mouse splenic lymphocytes. A relatively high dose of ConA induced a significantly higher mortality rate in the GnT-V Tg mice compared with the that in WT mice. The binding affinity of ConA to LSEC, which occurs in the first phase of ConA hepatitis, did not differ between the WT and GnT-V Tg mice. The results also revealed significant increases in hepatic macrophage infiltration in the GnT-V Tg mice liver compared with the WT mouse liver, prior to or following ConA injection. Notably, the gene expression of galectin-3, a hepatocyte and one of the major chemoattractants of macrophage, was increased in the Tg mice. These findings indicated that GnT-V-induced galectin-3 elevation recruited monocytes to the liver and resulted in an increased number of hepatic macrophages, ultimately leading to enhanced ConA-induced hepatitis in the Tg mice. The present study also observed that the depletion of macrophages inhibited and reduced the difference in the degree of ConA-induced hepatitis between the WT and GnT-V Tg mice. Considering these findings, the present study demonstrated that aberrant glycosylation, induced by GnT-V, increased hepatic macrophage infiltration and resulted in enhanced ConA-induced hepatitis.

In the liver, LSECs, Kupffer cells (hepatic macrophages), lymphocytes (T cells) and NK cells are involved in the immune response of ConA-induced hepatitis (5). Among these immune cells, T cells are critical in ConA-induced hepatitis (1,4,5). Therefore, to investigate the roles of GnT-V on T cell activation, splenic lymphocytes from WT and GnT-V Tg mice were stimulated with anti-CD3/CD28 antibodies or ConA *in vitro*. The GnT-V Tg mouse splenic lymphocytes produced lower levels of the IFN-γ Th1 cytokine and higher levels of the IL-10 Th2 cytokine compared with the WT mouse splenic lymphocytes. These findings were consistent with those of previous studies, which demonstrated that GnT-V-induced TCR oligosaccharide modification suppresses TCR signaling (22,23). However, these findings indicate that GnT-V tends to suppress inflammatory responses through suppression of T cell activation, which differ from the results of the present *in vivo* study.

ConA binds predominantly to LSECs within 15 min following intravenous injection. After 4 h, ConA begins to bind to hepatic macrophages (33), and activated lymphocytes are then trafficked towards hepatocytes, leading to inflammation (5,32). The present study hypothesized that the glycosylation differences between the LSECs of WT and GnT-V Tg mice may be important in the progression of ConA-induced hepatitis. To examine this hypothesis, differences in the lectin affinities of each mouse LSEC were investigated. It was found that ConA and L_4-PHA lectin bound equally to the WT and GnT-V Tg mouse LSECs, however, the expression of GnT-V was increased in the GnT-V Tg mice. Since levels of β1-6 GlcNAc branching are regulated by UDP-GlcNAc, a donor substrate of GnT-V (33), a change in the expression of GnT-V alone were insufficient to increase levels of β1-6 GlcNAc branching in the Tg mouse LSECs.

In response to these T cell and LSEC findings, the present study investigated hepatic macrophages as the main effector cell in the second phase of ConA-induced hepatitis (33,35). The hepatic macrophages were significantly increased in the

GnT-V Tg mice compared with the WT mice prior to and following ConA administration. It is understood that β1-6 GlcNAc branching extends repeated glycans of GlcNAc and galactose and results in a polylactosamine structure (36). Endogenous galectin-3 binds to this polylactosamine structure. Galectin-3 is a chemoattractant for monocytes and macrophages, which induces macrophage infiltration into the organs (35,37,38) and promotes inflammatory changes in various organs (35). Therefore, the polylactosamine structure induced in GnT-V Tg mice may increase the quantity of hepatic galectin-3. The present study also observed that the gene expression of galectin-3 was increased in the GnT-V Tg hepatocytes compared with the WT mouse hepatocytes. Therefore, GnT-V Tg mouse hepatocytes may produce higher quantities of galectin-3 than WT mouse hepatocytes. Increased hepatic galectin-3 in the GnT-V Tg mice may result in the elevated proportion of macrophages among the hepatic MNCs. In the present study, depletion of hepatic macrophages by clodronate-liposome infusion decreased the severity of ConA-induced hepatitis in the WT and GnT-V Tg mice and reduced the differences in liver injury between these mice. These results indicated that aberrant glycosylation by GnT-V elevated hepatic macrophage infiltration via an increase in hepatic galectin-3, exacerbating ConA-induced hepatitis. The reason for GnT-V-induced increases in hepatic galectin-3 and target glycoproteins for GnT-V in macrophages remains to be elucidated and its mechanisms require further investigation.

In conclusion, aberrant glycosylation by GnT-V led to increases in hepatic macrophage infiltration and enhanced ConA-induced hepatitis in mice. These findings indicate that the modulation of glycosylation may be a novel therapeutic target for immunity-associated acute hepatitis.

Acknowledgements

The present study was supported by Grants-in-Aid for Scientific Research (no. 21249038) and the Japan Society for the Promotion of Science (no. 24590972),.

References

1. Gantner F, Leist M, Lohse AW, Germann PG and Tiegs G: Concanavalin A-induced T-cell-mediated hepatic injury in mice: the role of tumor necrosis factor. Hepatology 21: 190-198, 1995.
2. Margalit M, Abu Gazala S, Alper R, *et al*: Glucocerebroside treatment ameliorates ConA hepatitis by inhibition of NKT lymphocytes. Am J Physiol Gastrointest Liver Physiol 289: G917-G925, 2005.
3. Takeda K, Hayakawa Y, Van Kaer L, Matsuda H, Yagita H and Okumura K: Critical contribution of liver natural killer T cells to a murine model of hepatitis. Proc Natl Acad Sci USA 97: 5498-5503, 2000.
4. Tiegs G, Hentschel J and Wendel A: A T cell-dependent experimental liver injury in mice inducible by concanavalin A J Clin Invest 90: 196-203, 1992.
5. Wang HX, Liu M, Weng SY, *et al*: Immune mechanisms of Concanavalin A model of autoimmune hepatitis. World J Gastroenterol 18: 119-125, 2012.
6. Yang MC, Chang CP and Lei HY: Endothelial cells are damaged by autophagic induction before hepatocytes in Con A-induced acute hepatitis. Int Immunol 22: 661-670, 2010.
7. Tsui TY, Obed A, Siu YT, *et al*: Carbon monoxide inhalation rescues mice from fulminant hepatitis through improving hepatic energy metabolism. Shock 27: 165-171, 2007.
8. Racanelli V and Rehermann B: The liver as an immunological organ. Hepatology 43: S54-S62, 2006.
9. Schrage A, Wechsung K, Neumann K, *et al*: Enhanced T cell transmigration across the murine liver sinusoidal endothelium is mediated by transcytosis and surface presentation of chemokines. Hepatology 48: 1262-1272, 2008.
10. Gove ME, Rhodes DH, Pini M, *et al*: Role of leptin receptor-induced STAT3 signaling in modulation of intestinal and hepatic inflammation in mice. J. Leukoc Biol 85: 491-496, 2009.
11. Takahashi K, Murakami M, Kikuchi H, Oshima Y and Kubohara Y: Derivatives of Dictyostelium differentiation-inducing factors promote mitogen-activated IL-2 production via AP-1 in Jurkat cells. Life Sci 88: 480-485, 2011.
12. Miller ML, Sun Y and Fu YX: Cutting edge: B and T lymphocyte attenuator signaling on NKT cells inhibits cytokine release and tissue injury in early immune responses. J Immunol 183: 32-36, 2009.
13. Boring L, Gosling J, Chensue SW, *et al*: Impaired monocyte migration and reduced type 1 (Th1) cytokine responses in C-C chemokine receptor 2 knockout mice. J Clin Invest 100: 2552-2561, 1997.
14. Kato M, Ikeda N, Matsushita E, Kaneko S and Kobayashi K: Involvement of IL-10, an anti-inflammatory cytokine in murine liver injury induced by Concanavalin A. Hepatol Res 20: 232-243, 2001.
15. Di Marco R, Xiang M, Zaccone P, *et al*: Concanavalin A-induced hepatitis in mice is prevented by interleukin (IL)-10 and exacerbated by endogenous IL-10 deficiency. Autoimmunity 31: 75-83, 1999.
16. Ohtsubo K and Marth JD: Glycosylation in cellular mechanisms of health and disease. Cell 126: 855-867, 2006.
17. Rademacher TW, Parekh RB and Dwek RA: Glycobiology. Annu Rev Biochem 57: 785-838, 1988.
18. Zhao Y, Sato Y, Isaji T, *et al*: Branched N-glycans regulate the biological functions of integrins and cadherins. FEBS J 275: 1939-1948, 2008.
19. Taniguchi N, Miyoshi E, Ko JH, Ikeda Y and Ihara Y: Implication of N-acetylglucosaminyltransferases III and V in cancer: gene regulation and signaling mechanism. Biochim Biophys Acta 1455: 287-300, 1999.
20. Lau KS and Dennis JW: N-Glycans in cancer progression. Glycobiology 18: 750-760, 2008.
21. Taniguchi N, Ihara S, Saito T, Miyoshi E, Ikeda Y and Honke K: Implication of GnT-V in cancer metastasis: a glycomic approach for identification of a target protein and its unique function as an angiogenic cofactor. Glycoconj J 18: 859-865, 2001.
22. Demetriou M, Granovsky M, Quaggin S and Dennis JW: Negative regulation of T-cell activation and autoimmunity by Mgat5 N-glycosylation. Nature 409: 733-739, 2001.
23. Li D, Li Y, Wu X, *et al*: Knockdown of Mgat5 inhibits breast cancer cell growth with activation of CD4+ T cells and macrophages. J. Immunol 180: 3158-3165, 2008.
24. Miyoshi E, Nishikawa A, Ihara Y, Gu J, *et al*: N-acetylglucosaminyltransferase III and V messenger RNA levels in LEC rats during hepatocarcinogenesis. Cancer Res 53: 3899-3902, 1993.
25. Miyoshi E, Ihara Y, Nishikawa A, *et al*: Gene expression of N-acetylglucosaminyltransferases III and V: a possible implication for liver regeneration. Hepatology 22: 1847-1855, 1995.
26. Kamada Y, Mori K, Matsumoto H, *et al*: N-Acetylglucosaminyltransferase V regulates TGF-beta response in hepatic stellate cells and the progression of steatohepatitis. Glycobiology 22: 778-787, 2012.
27. Terao M, Ishikawa A, Nakahara S, *et al*: Enhanced epithelial-mesenchymal transition-like phenotype in N-acetylglucosaminyltransferase V transgenic mouse skin promotes wound healing. J Biol Chem 286: 28303-28311, 2011.
28. Aicher WK, Fujihashi K, Yamamoto M, Kiyono H, Pitts AM and McGhee JR: Effects of the lpr/lpr mutation on T and B cell populations in the lamina propria of the small intestine, a mucosal effector site. Int Immunol 4: 959-968, 1992.
29. Kristensen DB, Kawada N, Imamura K, *et al*: Proteome analysis of rat hepatic stellate cells. Hepatology 32: 268-277, 2000.
30. Trobonjaca Z, Leithauser F, Moller P, Schirmbeck R and Reimann J: Activating immunity in the liver. I. Liver dendritic cells (but not hepatocytes) are potent activators of IFN-gamma release by liver NKT cells. J. Immunol 167: 1413-1422, 2001.
31. Shinzaki S, Iijima H, Fujii H, *et al*: Altered oligosaccharide structures reduce colitis induction in mice defective in beta-1,4-galactosyltransferase. Gastroenterology 142: 1172-1182, 2012.
32. Van Rooijen N and Sanders A: Liposome mediated depletion of macrophages: mechanism of action, preparation of liposomes and applications. J Immunol Methods 174: 83-93, 1994.

33. Knolle PA, Gerken G, Loser E, *et al*: Role of sinusoidal endothelial cells of the liver in concanavalin A-induced hepatic injury in mice. Hepatology 24: 824-829, 1996.
34. Sasai K, Ikeda Y, Fujii T, Tsuda T and Taniguchi N: UDP-GlcNAc concentration is an important factor in the biosynthesis of beta1,6-branched oligosaccharides: regulation based on the kinetic properties of N-acetylglucosaminyltransferase V. Glycobiology 12: 119-127, 2002.
35. Bacigalupo ML, Manzi M, Rabinovich GA and Troncoso MF: Hierarchical and selective roles of galectins in hepatocarcinogenesis, liver fibrosis and inflammation of hepatocellular carcinoma. World J Gastroenterol 19: 8831-8849, 2013.
36. Lee RT and Lee YC: Affinity enhancement by multivalent lectin-carbohydrate interaction. Glycoconj J 17: 543-551, 2000.
37. Sano H, Hsu DK, Yu L, *et al*: Human galectin-3 is a novel chemoattractant for monocytes and macrophages. J Immunol 165: 2156-2164, 2000.
38. Volarevic V, Milovanovic M, Ljujic B, *et al*: Galectin-3 deficiency prevents concanavalin A-induced hepatitis in mice. Hepatology 55: 1954-1964, 2012.

SCIENTIFIC REPORTS

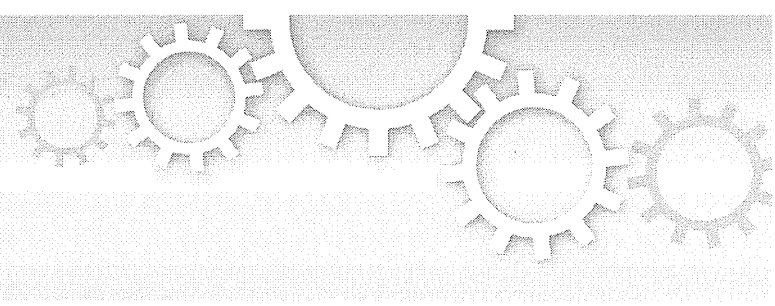

OPEN

SUBJECT AREAS:
BIOCHEMISTRY
GLYCOBIOLOGY

Received
16 September 2014

Accepted
14 January 2015

Published
5 February 2015

Correspondence and requests for materials should be addressed to J.G. (jgu@tohoku-pharm.ac.jp)

Loss of α1,6-fucosyltransferase suppressed liver regeneration: implication of core fucose in the regulation of growth factor receptor-mediated cellular signaling

Yuqin Wang[1], Tomohiko Fukuda[1], Tomoya Isaji[1], Jishun Lu[1], Wei Gu[1], Ho-hsun Lee[1], Yasuhito Ohkubo[2], Yoshihiro Kamada[3], Naoyuki Taniguchi[4], Eiji Miyoshi[3] & Jianguo Gu[1]

[1]Division of Regulatory Glycobiology, Tohoku Pharmaceutical University, Sendai, Miyagi, 981-8558, Japan, [2]Department of Radiopharmacy, Tohoku Pharmaceutical University, Sendai, Miyagi, 981-8558, Japan, [3]Department of Molecular Biochemistry and Clinical Investigation, Osaka University Graduate School of Medicine, Osaka, 565-0871, Japan, [4]Disease Glycomics Team, RIKEN, Wako, Saitama, 351-0198, Japan.

Core fucosylation is an important post-translational modification, which is catalyzed by α1,6-fucosyltransferase (Fut8). Increased expression of Fut8 has been shown in diverse carcinomas including hepatocarcinoma. In this study, we investigated the role of Fut8 expression in liver regeneration by using the 70% partial hepatectomy (PH) model, and found that Fut8 is also critical for the regeneration of liver. Interestingly, we show that the Fut8 activities were significantly increased in the beginning of PH (~4d), but returned to the basal level in the late stage of PH. Lacking Fut8 led to delayed liver recovery in mice. This retardation mainly resulted from suppressed hepatocyte proliferation, as supported not only by a decreased phosphorylation level of epidermal growth factor (EGF) receptor and hepatocyte growth factor (HGF) receptor in the liver of Fut8$^{-/-}$ mice *in vivo*, but by the reduced response to exogenous EGF and HGF of the primary hepatocytes isolated from the Fut8$^{-/-}$ mice. Furthermore, an administration of L-fucose, which can increase GDP-fucose synthesis through a salvage pathway, significantly rescued the delayed liver regeneration of Fut8$^{+/-}$ mice. Overall, our study provides the first direct evidence for the involvement of Fut8 in liver regeneration.

The adult liver has a remarkable capacity to regenerate, which makes it possible to use partial livers from living donors for transplantation. However, certain hepatic conditions, including cirrhosis, steatosis, and conditions due to old age, also have impaired liver regeneration that results in increased morbidity and mortality in response to liver transplantation[1]. Therefore, in the past decade, numerous studies have been focused on dissecting the molecular mechanisms underlying liver regeneration.

Seventy percent partial hepatectomy (PH) is the most common technique that is used to study the regeneration of liver. Namely, it describes a surgical procedure which removes 70% of liver mass in rodents (rats and mice). Due to the multi-lobed structure of the rodent liver, three of the five liver lobes (representing 70% of its liver mass) can be removed. The residual lobes enlarge and reconstitute the original size of the liver within 2 weeks[2,3]. Regeneration after PH is a complicated process. At the cellular level, it proceeds with the coordinated proliferation of all types of mature hepatic cells. Among these, it has been generally accepted that the restoration of liver volume depends mainly on the proliferation of hepatocytes[4]. This is not only because hepatocytes account for about 80% of liver weight and 70% of all liver cells, but also they are the first cells to enter into DNA synthesis and produce mitogenic signals for other hepatic cells[4,5]. Molecularly, PH triggers multiple intracellular signaling cascades (RAS/mitogen-activated protein kinase (MAPK) signaling, c-Met signaling, etc), leading to great changes in the expression of genes associated with cell proliferation[1,6]. The convergence of these signaling pathways has been reportedly mediated via epidermal growth factor receptor (EGFR) and hepatocyte growth factor receptor (HGFR, also called c-Met)[4]. Blocking the EGFR- or c-Met-mediated signaling pathway could cause a severe delay of liver

regeneration. In addition to the expression level of EGFR and c-Met proteins, it has been shown that the post-translational modification of these receptors such as ubiquitination, phosphorylation, and glycosylation also plays a crucial role in the regulation of these signaling pathways[7,8].

Fucosylation is one type of glycosylation. It describes the attachment of a fucose residue to *N*-glycans, *O*-glycans, and glycolipid catalyzed by a family of enzymes called fucosyltransferases (Futs)[9]. Among these, α1,6-fucosyltransferase (Fut8) is the only enzyme that catalyzes the transfer of a fucose from GDP-fucose to the innermost GlcNAc residue via α1,6-linkage to form core fucosylation in mammals as shown in Figure 1c. The enzymatic products, core fucosylated *N*-glycans, are widely distributed in a variety of glycoproteins and have been shown to play important roles in cell signaling. As examples, we previously showed that core fucosylation is crucial for the ligand binding affinity of TGF-β1 receptor[10], EGF receptor[11], and integrin α3β1[12]. Lacking the core fucose of these receptors led to a marked reduction in their ligand-binding ability and downstream signaling. Recently, our group found that a loss of core fucose on activin receptors resulted in an enhancement of the formation of activin receptor complexes, which constitutively activated intracellular signaling[13]. These studies indicate that core fucosylation is able to negatively or positively affect signaling pathways through regulation of receptor binding ability.

Abnormal expression of Fut8 has been pathologically correlated with diverse carcinomas including liver[14], ovarian[15], lung[16] and colorectal cancers[17]. Recently it was reported that core fucosylation on some glycoproteins, such as vitronectin, increased during liver regeneration after PH[18]. However, the underlying mechanisms remain poorly understood. Here, we investigated the role of Fut8 in liver regeneration and showed for the first time that core fucosylation is physiologically associated with the liver regeneration. In particular, we show that the liver regeneration was significantly inhibited in Fut8 deficient ($Fut8^{-/-}$) and Fut8 hetero ($Fut8^{+/-}$) mice as compared to wild type ($Fut8^{+/+}$) mice. It is intriguing that this effect could be attenuated by L-fucose supplementation in the $Fut8^{+/-}$ mice. Moreover, intracellular signaling analysis using primary hepatocytes isolated from $Fut8^{+/+}$ and $Fut8^{-/-}$ mice clearly demonstrated that Fut8 is important for the initiation of hepatocyte proliferation. Taken together, our data here provide novel insight for the function of core fucosylation in liver regeneration.

Results

70% PH induced the expression of Fut8. It has been reported that lacking N-acetylglucosaminyltransferase III suppressed the liver tumor progression and liver regeneration in mice, indicating the importance of glycosylation in liver[19]. In the present study, we investigated the roles of Fut8 in liver regeneration. Firstly, we chose to use HPLC to examine the enzyme activities of Fut8 by in the liver tissues at different time points after 70% PH, since the expression level of Fut8 in liver is much lower than that in other tissues under physiological conditions, and it is difficult to detect

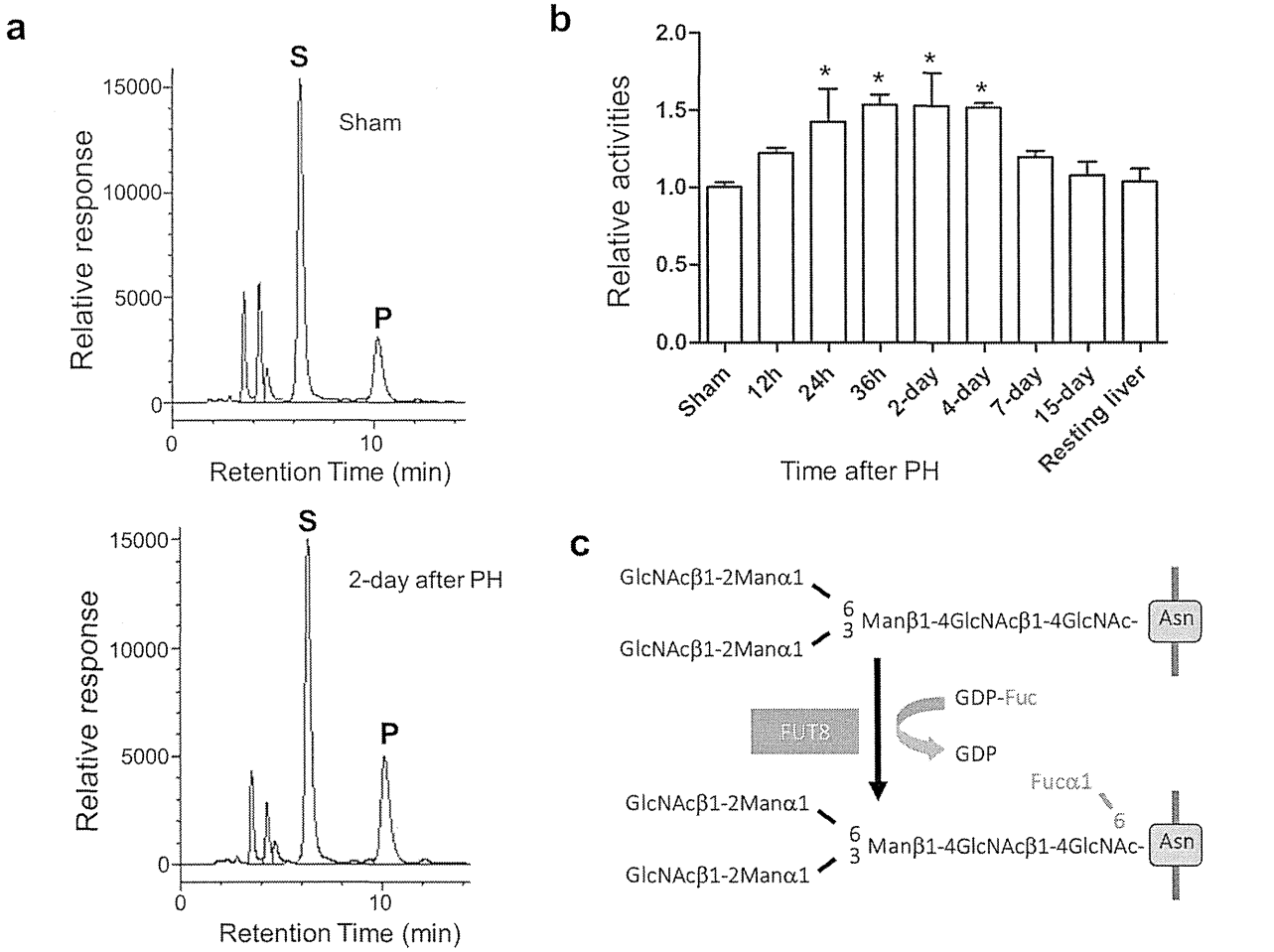

Figure 1 | The activities of Fut8 were increased after 70% partial hepatectomy (PH). The liver tissues were harvested for the determination of enzyme activities at indicated times as described in "Methods". (a) A representative elution pattern on HPLC for Fut8 activities in $Fut8^{+/+}$ mouse with (left panel) or without (right panel) PH. S: substrate; P: product. (b) The quantitative assay for enzyme activities in $Fut8^{+/+}$ mice after PH. *, $P < 0.05$, compared to the group without PH (sham), which was set as 1, n = 3. (c) Reaction for synthesis of α1,6-fucose.

endogenous Fut8 by anti-Fut8 antibody even after the induction by PH. As shown in Figure 1a and 1b, the Fut8 activities were increased in the first 4 days after operation, and returned to normal levels after liver mass is restored. The similar pattern was also observed in mRNA expression confirmed by RT-PCR (data not shown). On the other hand, the expression levels of L-fucosidase after PH were not changed confirmed by RT-PCR (data not shown). These data indicated that the induction of Fut8 expression might be required for liver regeneration.

Loss of Fut8 inhibited recovery of liver mass after a two-third liver resection. To testify the hypothesis above, we performed a 70% PH on both $Fut8^{+/+}$ and $Fut8^{-/-}$ mice, and analyzed the restoration of their livers. Interestingly, the regeneration index calculated as an increase in liver-to-body weight ratio was significantly lower in $Fut8^{-/-}$ mice than that in $Fut8^{+/+}$ mice (Figure 2a). Furthermore, a decrease in liver regeneration was also observed in the $Fut8^{+/-}$ mice during the first 2 days (Figure 2b). The results above indicated that the liver regeneration was inhibited in $Fut8^{-/-}$ mice as compared to $Fut8^{+/+}$ mice.

Liver regeneration was achieved by the coordinated proliferation of all types of mature hepatic cells[2]. Consistent with the results above, quantitative assessment of Ki67 by immunostaining revealed little difference between $Fut8^{-/-}$ and $Fut8^{+/+}$ mice without PH, while, the percentage of Ki67 positive versus TO-PRO-3 iodide positive cells in the livers of $Fut8^{-/-}$ mice were markedly less than that in $Fut8^{+/+}$ mice at day 2 after PH (Figure 3a and 3b). These differences in cell proliferation were further reflected by the cell proliferation signaling. As shown in figure 3c, the phosphorylation levels of ERK were remarkably lower in the $Fut8^{-/-}$ mice as compared with $Fut8^{+/+}$ mice, although the MAPK signaling pathways were activated by PH in both $Fut8^{+/+}$ and $Fut8^{-/-}$ mice. Overall, these data indicated that the delayed liver recovery in $Fut8^{-/-}$ mice resulted from the lower cell proliferation.

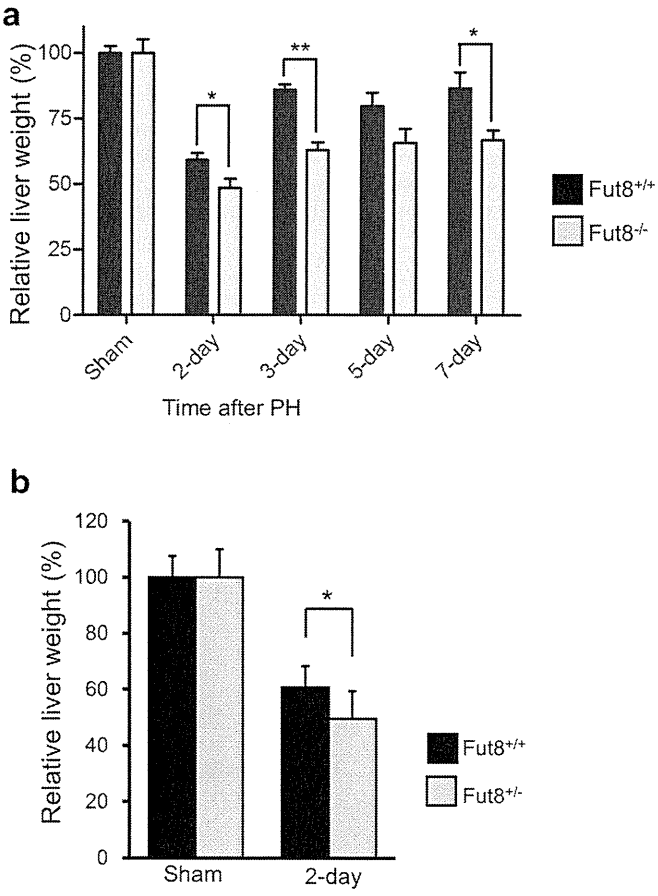

Figure 2 | Fut8 expression was required for liver regeneration after PH. 7- to 8-week-old mice were surgically resected as described in "Methods", and then the livers were harvested at the indicated times. (a) Relative liver weight (liver vs whole body) at the indicated times after 70% PH. The sham group was set as 100%. Each set of the reported data was obtained from at least 5 individuals of $Fut8^{+/+}$ and $Fut8^{-/-}$ mice. *, $P < 0.05$; **, $P < 0.01$. (b) Comparison of relative weight at 2 days after PH between $Fut8^{+/+}$ and $Fut8^{+/-}$ mice (C57BL/6 genetic background). Each data was obtained from at least 8 individuals. *, $P < 0.05$, compared with the $Fut8^{+/+}$ mice.

L-fucose administration in $Fut8^{+/-}$ mice attenuated the inhibitory effect in cell proliferation as described above. GDP-fucose is the donor for fucosyltransferases. It is known that two pathways for the synthesis of GDP-fucose in mammalian cells, the GDP-mannose-dependent *de novo* pathway and the free fucose-dependent salvage pathway[20]. And what is more, administration of oral L-fucose, an enhancement of the salvage pathway, has been proven useful for correction of fucosylation defects in leukocyte adhesion deficiency type II (LAD II) patients[21]. To determine whether enhancing GDP-fucose salvage pathway could complement the delayed liver regeneration of the $Fut8^{+/-}$ mice as described above, we checked the effects of L-fucose supplementation in the $Fut8^{+/-}$ mice. Interestingly, an oral administration of L-fucose significantly accelerated liver regeneration of the $Fut8^{+/-}$ mice, but did not affect sham mice (Figure 4a). Consistently, in contrast to the little difference in the case of livers without 70% PH, immunostaining with Ki67 showed the ratio of $Ki67^{+}$ to TO-PRO-3 $iodide^{+}$ cells in the livers treated by PH were clearly increased after L-fucose administration (Figure 4b and 4c). Moreover, as shown in figure 4d and 4e, the phosphorylation levels of ERK and EGFR were induced in $Fut8^{+/-}$ mice after PH. Furthermore, the L-fucose administration up-regulated their phosphorylation levels, although there was no significant difference between the mice treated with or without L-fucose by statistical analysis. These results further suggest that Fut8 and its products are important for cell proliferation in liver regeneration.

The intracellular signaling was inhibited in the $Fut8^{-/-}$ primary hepatocytes upon stimulation with EGF or HGF. The EGF and HGF are major mitogens for hepatocytes in the regenerating liver. Lacking EGFR or c-Met in mice resulted in the liver regeneration abnormalities[22,23]. To determine whether the delayed liver recovery in the $Fut8^{-/-}$ mice is due to the impaired EGFR and/or c-Met signaling, we tested the expression levels of the key effectors in these signaling pathways. As shown in Figure 5a and b, although c-Met and EGFR associated signaling pathways were activated in both $Fut8^{+/+}$ and $Fut8^{-/-}$ mice 2 days post PH, the levels of phosphorylated c-Met (Tyr1234/5) and EGFR (Tyr1068) in $Fut8^{-/-}$ mice were obviously lower than that in $Fut8^{+/+}$ mice. These results indicated that loss of Fut8 impaired EGFR and c-Met associated signaling during liver regeneration.

To further corroborate the results above *in vitro*, we examined the downstream signaling cascades of EGF or HGF using the primary hepatocytes isolated from $Fut8^{+/+}$ and $Fut8^{-/-}$ mice. Consistently, the treatments with EGF or HGF significantly increased the expression levels of phosphorylated ERK and AKT in the $Fut8^{+/+}$ cells. However, these increases were greatly suppressed in the $Fut8^{-/-}$ cells (Figure 5d and e). The results above clearly demonstrated that the impaired regeneration in $Fut8^{-/-}$ livers was due, at least mainly, to the down-regulated EGFR- and c-Met-mediated signalings in hepatocytes.

Discussion

In the present study, we used a well-established regeneration model, to investigate the functions of Fut8 in liver regeneration, and found

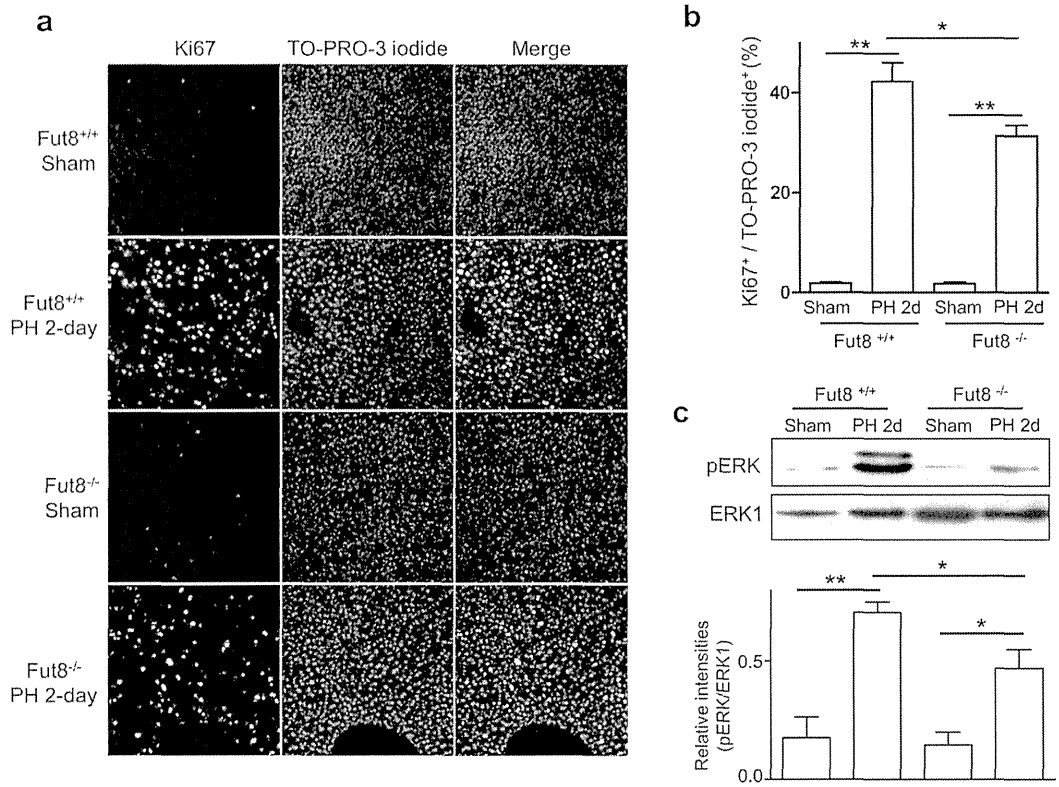

Figure 3 | Cell proliferation was suppressed in the livers of Fut8$^{-/-}$ mice. (a) Immunostaining for liver tissues (10 μm frozen section) of Fut8$^{+/+}$ and Fut8$^{-/-}$ mice using anti-Ki67 antibody (200 × field). The positive cells of the immunostaining were labeled with the green spots (left panel), and the nuclei were labeled by TO-PRO-3 iodide (red spots, middle panel). (b) The quantitative data were obtained from at least 3 mice in each group. **, $P < 0.01$. (c) Equal protein of liver lysates at day 2 after PH were separated by 10% SDS-PAGE and blotted with anti-phospho-ERK and anti-ERK1 antibodies. The quantitative data were obtained from 3 mice in each group. *, $P < 0.05$, **, $P < 0.01$.

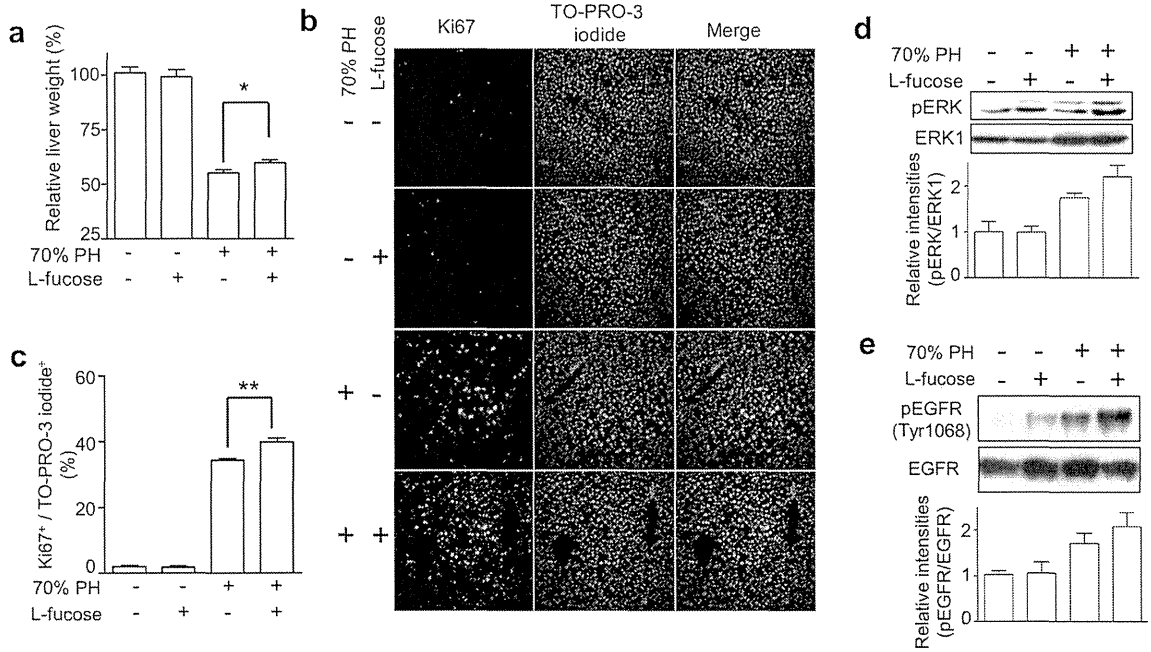

Figure 4 | L-fucose supplementation attenuated the decreased regeneration of Fut8$^{+/-}$ mice. (a) Relative liver weight (liver vs whole body) at 2-day after PH in Fut8$^{+/-}$ mice with or without administration of L-fucose. Prior to operation, 6-week old Fut8$^{+/-}$ mice were administrated with L-fucose at 4 g/L in water for 12 days, and then the livers were harvested at 48 hours after PH. The sham group without L-fucose treatment was set as 100%. *, $P < 0.05$, compared with the mice without L-fucose treatment (n > 10 mice). (b) Immunostaining for liver tissues using anti-Ki67 antibody (200 × field). (c) The quantitative data were obtained from at least 3 mice in each group, *, $P < 0.05$. Equal protein of liver lysates at day 2 after PH were separated by SDS-PAGE (10% for pERK/ERK1, 7% for pEGFR/EGFR) and blotted with anti-phospho-ERK and anti-ERK1 antibodies. The quantitative data were obtained from 3 mice in each group.

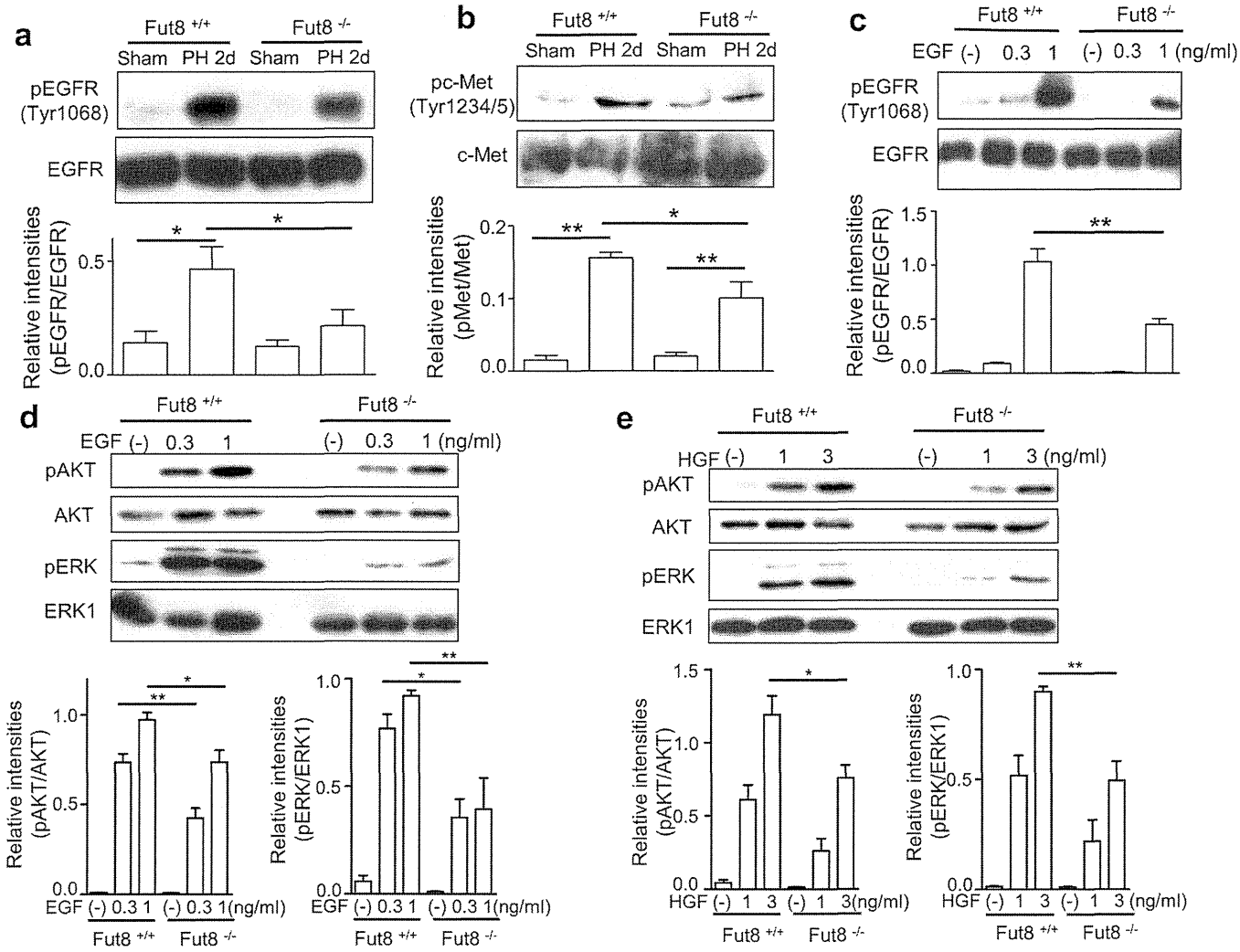

Figure 5 | Intracellular signaling was suppressed in Fut8$^{-/-}$ mice upon either PH or EGF and HGF stimulation. 8-week-old Fut8$^{+/+}$ or Fut8$^{-/-}$ mice were surgically resected as described in "Methods", and then the livers were harvested at 2 days. The liver homogenates were separated by 7% SDS-PAGE and blotted with anti-EGFR and anti-phospho-EGFR antibodies (a), and anti-c-Met and anti-phospho-c-Met antibodies (b). The quantitative data were obtained from 3 mice in each group. *, $P < 0.05$, **, $P < 0.01$. The primary hepatocytes isolated from 8-week old Fut8$^{+/+}$ and Fut8$^{-/-}$ mice were cultured in DMEM containing with 10% FBS for 12 h, and then cultured under DMEM containing with 0.1% FBS for 24 hours. After the starvation, these cells were stimulated with or without EGF at indicated concentrations for 5 min (c and d), or HGF at indicated concentrations for 10 min (e). The cell lysates were immunoblotted with anti-pEGFR and anti-EGFR, anti-pAKT and anti-AKT antibodies, anti-pERK and anti-ERK1 antibodies. The quantitative data were obtained from at least 3 independent experiments, *, $P < 0.05$, **, $P < 0.0$ 1.

the following: i) The expression of Fut8 was markedly up-regulated during the regenerating process in the Fut8$^{+/+}$ mice; ii) the liver regeneration was greatly inhibited in Fut8$^{-/-}$ mice compared to Fut8$^{+/+}$ mice; iii) L-fucose supplementation could reverse the delayed regeneration in Fut8$^{+/-}$ mice; and, iv) the responses to growth factors such as EGF and HGF, were decreased in Fut8 deficient hepatocytes compared to wild-type hepatocytes. Overall, this study marks the first clear demonstration of the biological functions of Fut8 in the liver, suggesting that core fucosylation plays important roles in liver regenerating progression as shown in Fig. 6.

Liver regeneration after PH is a complicated process with the coordinated proliferation of all types of mature hepatic cells, which involves numerous molecules and signaling pathways[1,2,6,24]. Among these, the EGFR-mediated signaling has been reported to be critical for liver regeneration[24]. Lacking EGFR in hepatocytes increased the mouse mortality rate after PH, and delayed the hepatocyte proliferation[23], although little effect was observed on liver function. We have previously shown that core fucosylation on EGFR is required for its binding to EGF and downstream signaling in embryonic fibroblast cells[11]. Therefore, it is reasonable to consider that the delayed liver recovery of Fut8$^{-/-}$ mice could be attributed, at least mainly, to the loss of the core fucosylation on the EGFR protein (Figure 5c and d). In agreement with this hypothesis, we found here that knockout of Fut8 led to an inhibition of the EGFR-mediated signaling cascade both *in vivo* and *in vitro*.

In addition to EGFR, c-Met has also been shown to play an irreplaceable role in liver regeneration. c-Met gene deficient or suppressed by shRNAs significantly inhibited the proliferation of hepatocytes after PH[22,25,26]. In the present study, we found that knockout of Fut8 also attenuated the response to an HGF stimulus in primary hepatocytes (Figure 5e). Since c-Met is also a core fucosylated protein which had been confirmed by using human cell lines (data not shown), one possibility for this attenuated response is that like EGFR, the core fucosylation on c-Met may be necessary for its ligand binding and downstream signaling as well. Obviously, we could not exclude other possibilities. Recently, Tobias Speicher et al. reported that the β1-integrin knockout or knockdown in mice inhibited liver regeneration by impairing the ligand-induced

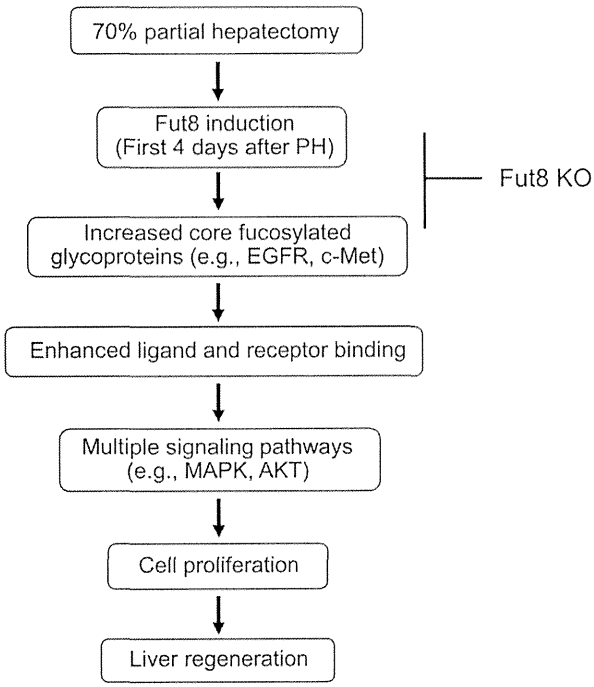

Figure 6 | Proposed molecular mechanisms for the delayed liver regeneration in Fut8$^{-/-}$ mice. It is well known that the 70% partial hepatectomy could activate several cell proliferation associated signaling pathways including Ras/MAPK signaling, c-Met signaling, and Akt/mammalian targets of rapamycin (mTOR) signaling, which up-regulate the cell proliferation, and consequently lead to the restoration of liver. Loss of core fucosylation on growth factor receptors such as EGFR and c-Met may alter their conformation and impair their ligand binding, thereby inhibiting their downstream signalings, and ultimately suppressing the cell proliferation. Overall, a loss of Fut8 gene results in a decrease in liver regeneration.

phosphorylation of EGFR and c-Met, as well as their downstream signalings[27]. Considering also that α3β1 integrins were highly modified by Fut8 and loss of core fucosylation could result in the malfunction of β1-integrin[12], Fut8 may also affect the c-Met-mediated signaling in the liver regeneration by regulating the core fucosylation status of β1-integrin. Further investigation is required to confirm the hypotheses above.

Increasing evidence indicated the importance of core fucosylation in protein-protein interaction, and we proposed here that Fut8 may affect the liver regeneration through modulating some associated receptor-ligand bindings. However, the mechanistic roles of Fut8 underlying the protein-protein interaction remain poorly understood. Recently, two research teams determined the complex structures of glycosylated FcγRIIIa and human core fucosylated or afucosylated Fc of IgG[28,29]. Interestingly, the crystal structures indicated that core fucose depletion increased the incidence of the active conformation of the Tyr-296 of Fc, and thereby accelerated the formation of the high-affinity complex with its receptor. These findings clearly explained why the lack of a core fucose on IgG could greatly enhance antibody-dependent cell-mediated cytotoxicity as previously reported[30,31]. From a more general viewpoint, these studies provide direct evidence for the mechanistic roles of Fut8 in different biological processes, where the attachment of core fucose leads to an alteration of glycoprotein conformation, which determines its protein dynamics coupled with the selection of protein-protein interactions and complex formation, and consequently affects the intracellular signaling pathways.

The excellent results of liver transplantation have led to an increasing number of patients on the waiting list, while the number of liver donors remains stable[1,32]. Studies on potential hepatoprotective factors in liver injury may contribute to increasing the success ratio of liver transplantation. Here, we showed that liver regeneration is significantly inhibited in Fut8$^{-/-}$ mice. Moreover, L-fucose administration could partially complement the delayed liver recover in Fut8$^{+/-}$ mice. However, it had no effect on the liver growth of the Fut8$^{+/-}$ sham mice, so we hypothesize that Fut8 exerts its regulatory functions in the liver only after some stimulus such as 70% PH. Clearly, it needs to confirm this idea and elucidate the underlying mechanisms in future. Nevertheless, the current study provides clear evidence for the effect of L-fucose supplementation on liver regeneration in mice and indicates the important role of Fut8 in liver regeneration.

Methods

Mice. The Fut8-deficient mice line used for these studies has been described previously[10,33]. Male mice on an ICR background at 6 to 8 weeks of age were used for the experiments in the present study, comparing Fut8$^{-/-}$ animals with Fut8$^{+/+}$ littermates. Mice were housed in a temperature-controlled room with a 12-h dark/12-h light cycle. Food and water were provided *ad libitum*. The present study was approved by the Institutional Animal Care and Use Committee of Tohoku Pharmaceutical University, Japan.

70% partial hepatectomy. All experiments were carried out in accordance with relevant guidelines and regulations. For liver regeneration studies, 7- to 8- week-old mice were anesthetized with pentobarbital sodium and subjected to mid-ventral laparotomy with a two-third liver resection, as previously described[34,35]. The left and median liver lobes were surgically resected without injuring the remaining liver tissue. The removed parts represented the resting liver. At least three mice from each group were euthanized at each analysis time point. For L-fucose (Nacalai tesque Inc.) supplementation, 6-week-Fut8$^{+/-}$ mice were orally administrated with L-fucose (4 g/L in water) for 12 days prior to partial hepatectomy (PH), and then the livers were harvested at 48 h after operation.

Immunostainings. The hepatic lobules were assessed based on 10 μm frozen sections. Proliferative cells in the liver were detected through immunostaining with a monoclonal antibody recognizing Ki67 (Abcam), and examined with Olympus confocal laser scanning microscope (Olympus).

Cell culture. Primary hepatocytes of 8-week old mice were isolated using the standard method of *in situ* collagenase (Gibco) perfusion and digestion of liver with low-speed centrifugation (50 g, 1 min), as previously reported[36,37]. Isolated cells were plated on collagen type I-coated dishes in Dulbecco's modified Eagle's medium (DMEM) with 10% (v/v) fetal bovine serum (FBS), 100 IU/mL penicillin, and 100 μg/ml streptomycin. Hepatocytes were incubated for 6 h at 37°C in a humidified atmosphere with 95% air and 5% CO_2, allowing for cell attachment to the plate. The medium was then changed, which involved replacement by 0.1% FBS contained DMEM with or without EGF or HGF for stimulation at indicated times.

Western blotting analyses. Total protein was isolated from frozen liver tissue and cultured cells with TBS (20 mM Tris, 150 mM NaCl, PH 7.4) containing 1% triton X-100. Protein concentration was measured using a bicinchoninic acid protein assay kit (Thermo Scientific). Equal protein samples were separated by SDS-PAGE and then transferred onto nitrocellulose or polyvinylidinedifluoride (Millipore) membranes. After blocking with 5% skim milk, the membranes were incubated with specific antibodies against the indicated antibodies at 4°C overnight, followed by incubation with horseradish peroxidase-conjugated secondary antibody. Immunoreactivity was visualized by HRP substrate peroxide solution (Millipore). The related antibodies that are used included ERK1 (BD), phospho-ERK, phospho-AKT, AKT, phospho-Met (Tyr1234/5), c-Met, phospho-EGFR (Tyr1068), EGFR, rabbit IgG (Cell Signaling) and mouse IgG (Sigma).

Enzyme activity assays for Fut8. Frozen liver tissues were homogenized in TBS containing 1% protease inhibitor cocktail (Nacalai tesque Inc.). After centrifugation at 900 g for 10 min, the supernatant was collected for enzyme activity assays. Each sample containing 800 μg of total protein was centrifuged at 105,000 g for 1 h, then the pellet was resuspended in 0.1 M MES-NaOH (PH 7.0) for reactions. Equal amounts of protein were used in Fut8 activity assays. The specific activities of Fut8 were determined using a substrate, 4-(2-pyridylamino)-butyl-amine (PABA)-labeled GlcNAcβ1-2Manα1-6(GlcNAcβ1-2Mana1-3)Manβ1-4GlcNAcβ1-4GlcNAc-Asn (GnGn-Asn-PABA). Each assay used 2 mM of acceptor substrate and 2 mM GDP-L-fucose as a donor (in 10 μl of total reaction solution). The reactions were terminated by boiling after 2 h of incubation at 37°C, and the reaction mixtures were centrifuged at 10,000 g for 10 min. The result supernatants were applied to high-performance liquid chromatography (HPLC) equipped with a TSK-gel, ODS-80TM column (4.6 × 150 mm) in order to separate and quantitate the products. Elution was performed isocratically at 55°C using a 20 mM acetate buffer (pH 4.0) containing 0.15% butanol. The column eluate was monitored for fluorescence using a detector operating at excitation and emission wavelengths of 320 and 400 nm, respectively. The activities

of endogenous Fut8 were measured by HPLC, expressed as the pmol of fucose transferred/h/mg of proteins[38].

Statistical analysis. Results are given as the mean ± standard error of the mean (SEM). The data were analyzed using Prism 5.0 software (GraphPad Software Inc.). Comparisons were carried out using 2-tailed Mann-Whitney tests and/or a Tukey's Multiple Comparison test. A P value of less than 0.05 was considered significant.

1. Taub, R. Liver regeneration: from myth to mechanism. *Nat. Rev. Mol. Cell Biol.* **5**, 836–847 (2004).
2. Michalopoulos, G. K. Liver regeneration. *J. Cell Physil.* **213**, 286–300 (2007).
3. Michalopoulos, G. K. & DeFrances, M. Liver regeneration. *Adv. Biochem. Eng. Biotechnol.* **93**, 101–134 (2005).
4. Michalopoulos, G. K. Advances in liver regeneration. *Expert Rev. Gastroenterol. Hepatol.* **8**, 897–907 (2014).
5. Si-Tayeb, K., Lemaigre, F. P. & Duncan, S. A. Organogenesis and development of the liver. *Dev. Cell* **18**, 175–189 (2010).
6. Fausto, N., Campbell, J. S. & Riehle, K. J. Liver regeneration. *Hepatology* **43**, S45–53 (2006).
7. Boscher, C., Dennis, J. W. & Nabi, I. R. Glycosylation, galectins and cellular signaling. *Curr. Opin. Cell Biol.* **23**, 383–392 (2011).
8. Snider, N. T. & Omary, M. B. Post-translational modifications of intermediate filament proteins: mechanisms and functions. *Nat. Rev. Mol. Cell Biol.* **15**, 163–177 (2014).
9. Haltiwanger, R. S. & Lowe, J. B. Role of glycosylation in development. *Annu. Rev. Biochem.* **73**, 491–537 (2004).
10. Wang, X. *et al.* Dysregulation of TGF-beta1 receptor activation leads to abnormal lung development and emphysema-like phenotype in core fucose-deficient mice. *Proc. Natl. Acad. Sci. U S A* **102**, 15791–15796 (2005).
11. Wang, X. *et al.* Core fucosylation regulates epidermal growth factor receptor-mediated intracellular signaling. *J. Biol. Chem.* **281**, 2572–2577 (2006).
12. Zhao, Y. *et al.* Deletion of core fucosylation on alpha3beta1 integrin down-regulates its functions. *J. Biol. Chem.* **281**, 38343–38350 (2006).
13. Gu, W. *et al.* alpha1,6-Fucosylation regulates neurite formation via the activin/phospho-Smad2 pathway in PC12 cells: the implicated dual effects of Fut8 for TGF-beta/activin-mediated signaling. *FASEB J.* **27**, 3947–3958 (2013).
14. Hutchinson, W. L., Du, M. Q., Johnson, P. J. & Williams, R. Fucosyltransferases: differential plasma and tissue alterations in hepatocellular carcinoma and cirrhosis. *Hepatology* **13**, 683–688 (1991).
15. Takahashi, T. *et al.* alpha1,6fucosyltransferase is highly and specifically expressed in human ovarian serous adenocarcinomas. *Int. J. Cancer* **88**, 914–919 (2000).
16. Chen, C. Y. *et al.* Fucosyltransferase 8 as a functional regulator of nonsmall cell lung cancer. *Proc. Natl. Acad. Sci. U S A* **110**, 630–635 (2013).
17. Muinelo-Romay, L. *et al.* Expression and enzyme activity of alpha(1,6)fucosyltransferase in human colorectal cancer. *Int. J. Cancer* **123**, 641–646 (2008).
18. Sano, K. *et al.* Survival signals of hepatic stellate cells in liver regeneration are regulated by glycosylation changes in rat vitronectin, especially decreased sialylation. *J. Biol. Chem.* **285**, 17301–17309 (2010).
19. Yang, X., Tang, J., Rogler, C. E. & Stanley, P. Reduced hepatocyte proliferation is the basis of retarded liver tumor progression and liver regeneration in mice lacking N-acetylglucosaminyltransferase III. *Cancer Res.* **63**, 7753–7759 (2003).
20. Becker, D. J. & Lowe, J. B. Fucose: biosynthesis and biological function in mammals. *Glycobiology* **13**, 41R–53R (2003).
21. Hidalgo, A. *et al.* Insights into leukocyte adhesion deficiency type 2 from a novel mutation in the GDP-fucose transporter gene. *Blood* **101**, 1705–1712 (2003).
22. Borowiak, M. *et al.* Met provides essential signals for liver regeneration. *Proc. Natl. Acad. Sci. U S A* **101**, 10608–10613 (2004).
23. Natarajan, A., Wagner, B. & Sibilia, M. The EGF receptor is required for efficient liver regeneration. *Proc. Natl. Acad. Sci. U S A* **104**, 17081–17086 (2007).
24. Bohm, F., Kohler, U. A., Speicher, T. & Werner, S. Regulation of liver regeneration by growth factors and cytokines. *EMBO Mol. Med.* **2**, 294–305 (2010).
25. Paranjpe, S. *et al.* Cell cycle effects resulting from inhibition of hepatocyte growth factor and its receptor c-Met in regenerating rat livers by RNA interference. *Hepatology* **45**, 1471–1477 (2007).
26. Huh, C. G. *et al.* Hepatocyte growth factor/c-met signaling pathway is required for efficient liver regeneration and repair. *Proc. Natl. Acad. Sci. U S A* **101**, 4477–4482 (2004).
27. Speicher, T. *et al.* Knockdown and knockout of beta1-integrin in hepatocytes impairs liver regeneration through inhibition of growth factor signalling. *Nat. Commun.* **5**, 3862 (2014).
28. Ferrara, C. *et al.* Unique carbohydrate-carbohydrate interactions are required for high affinity binding between FcgammaRIII and antibodies lacking core fucose. *Proc. Natl. Acad. Sci. U S A* **108**, 12669–12674 (2011).
29. Mizushima, T. *et al.* Structural basis for improved efficacy of therapeutic antibodies on defucosylation of their Fc glycans. *Genes Cells* **16**, 1071–1080 (2011).
30. Okazaki, A. *et al.* Fucose depletion from human IgG1 oligosaccharide enhances binding enthalpy and association rate between IgG1 and FcgammaRIIIa. *J. Mol. Biol.* **336**, 1239–1249 (2004).
31. Shinkawa, T. *et al.* The absence of fucose but not the presence of galactose or bisecting N-acetylglucosamine of human IgG1 complex-type oligosaccharides shows the critical role of enhancing antibody-dependent cellular cytotoxicity. *J. Biol. Chem.* **278**, 3466–3473 (2003).
32. Jimenez-Romero, C. *et al.* Using old liver grafts for liver transplantation: Where are the limits? *World J. Gastroenterol.* **20**, 10691–10702 (2014).
33. Fukuda, T. *et al.* Alpha1,6-fucosyltransferase-deficient mice exhibit multiple behavioral abnormalities associated with a schizophrenia-like phenotype: importance of the balance between the dopamine and serotonin systems. *J. Biol. Chem.* **286**, 18434–18443 (2011).
34. Gao, L. *et al.* Reticulon 4B (Nogo-B) facilitates hepatocyte proliferation and liver regeneration in mice. *Hepatology* **57**, 1992–2003 (2013).
35. Mitchell, C. & Willenbring, H. A reproducible and well-tolerated method for 2/3 partial hepatectomy in mice. *Nat. Protoc.* **3**, 1167–1170 (2008).
36. Tokairin, T. *et al.* A highly specific isolation of rat sinusoidal endothelial cells by the immunomagnetic bead method using SE-1 monoclonal antibody. *J. Hepatol.* **36**, 725–733 (2002).
37. Maher, J. J., Bissell, D. M., Friedman, S. L. & Roll, F. J. Collagen measured in primary cultures of normal rat hepatocytes derives from lipocytes within the monolayer. *J. Clin. Invest.* **82**, 450–459 (1988).
38. Uozumi, N. *et al.* Purification and cDNA cloning of porcine brain GDP-L-Fuc:N-acetyl-beta-D-glucosaminide alpha1-->6fucosyltransferase. *J. Biol. Chem.* **271**, 27810–27817 (1996).

Acknowledgments

We thank Dr. Lucas Veillon (Tohoku Pharmaceutical University) for his assistance in language modification. This work was partly supported by a Grant-in-Aid for Scientific Research (21370059 to J.G.; 24590087 to T.F.; 24570169 to T.I.), for Challenging Exploratory Research (23651196 to J.G.) from the Japan Society for the Promotion of Science; by a grant from the Scientific Research on Innovative Areas (23110002 to J.G.) and the Strategic Research Foundation Grant-aided Project for Private Universities from the Ministry of Education, Culture, Sports, Science and Technology of Japan.

Author contributions

Y.W. and T.F. performed the all experiments. J.G. designed the project. Y.O., Y.K. and E.M. performed 70% hepatectomy. T.I., G.W. and H.L. analyzed cellular signaling. Y.W., T.F., J.L., N.T. and J.G. analyzed the data. Y.W. and J.G. wrote the manuscript with J.L. All authors discussed the results and commented on the manuscript.

Additional information

Competing financial interests: The authors declare no competing financial interests.

How to cite this article: Wang, Y. *et al.* Loss of α1,6-fucosyltransferase suppressed liver regeneration: implication of core fucose in the regulation of growth factor receptor-mediated cellular signaling. *Sci. Rep.* 5, 8264; DOI:10.1038/srep08264 (2015).

Hum Genet (2015) 134:279–289
DOI 10.1007/s00439-014-1520-7

ORIGINAL INVESTIGATION

Genome-wide association study identifies a *PSMD3* variant associated with neutropenia in interferon-based therapy for chronic hepatitis C

Etsuko Iio · Kentaro Matsuura · Nao Nishida · Shinya Maekawa · Nobuyuki Enomoto · Mina Nakagawa · Naoya Sakamoto · Hiroshi Yatsuhashi · Masayuki Kurosaki · Namiki Izumi · Yoichi Hiasa · Naohiko Masaki · Tatsuya Ide · Keisuke Hino · Akihiro Tamori · Masao Honda · Shuichi Kaneko · Satoshi Mochida · Hideyuki Nomura · Shuhei Nishiguchi · Chiaki Okuse · Yoshito Itoh · Hitoshi Yoshiji · Isao Sakaida · Kazuhide Yamamoto · Hisayoshi Watanabe · Shuhei Hige · Akihiro Matsumoto · Eiji Tanaka · Katsushi Tokunaga · Yasuhito Tanaka

Received: 2 October 2014 / Accepted: 8 December 2014 / Published online: 17 December 2014

Abstract Cytopenia during interferon-based (IFN-based) therapy for chronic hepatitis C (CHC) often necessitates reduction of doses of drugs and premature withdrawal from therapy resulting in poor response to treatment. To identify genetic variants associated with IFN-induced neutropenia, we conducted a genome-wide association study (GWAS) in 416 Japanese CHC patients receiving IFN-based therapy. Based on the results, we selected 192 candidate single nucleotide polymorphisms (SNPs) to carry out a replication analysis in an independent set of 404 subjects. The SNP rs2305482, located in the intron region of the *PSMD3* gene on chromosome 17, showed a strong association when the results of GWAS and the replication stage were combined (OR = 2.18, $P = 3.05 \times 10^{-7}$ in the allele frequency model). Logistic regression analysis showed that rs2305482 CC and neutrophil count at baseline were independent predictive factors for IFN-induced neutropenia (OR = 2.497, $P = 0.0072$ and OR = 0.998, $P < 0.0001$, respectively). Furthermore, rs2305482 genotype was associated with the doses of pegylated interferon (PEG-IFN) that could be tolerated in hepatitis C virus genotype 1-infected patients treated with PEG-IFN plus ribavirin, but not with treatment efficacy. Our results suggest that genetic

E. Iio and K. Matsuura equally contributed to this work (shared first authorship).

Electronic supplementary material The online version of this article (doi:10.1007/s00439-014-1520-7) contains supplementary material, which is available to authorized users.

E. Iio · K. Matsuura · Y. Tanaka (✉)
Department of Virology and Liver Unit, Nagoya City University Graduate School of Medical Sciences, Kawasumi, Mizuho, Nagoya 467-8601, Japan
e-mail: ytanaka@med.nagoya-cu.ac.jp

E. Iio · K. Matsuura
Department of Gastroenterology and Metabolism, Nagoya City University Graduate School of Medical Sciences, Nagoya 467-8601, Japan

N. Nishida · N. Masaki
The Research Center for Hepatitis and Immunology, National Center for Global Health and Medicine, Ichikawa 272-8516, Japan

N. Nishida · K. Tokunaga
Department of Human Genetics, Graduate School of Medicine, The University of Tokyo, Tokyo 113-0033, Japan

S. Maekawa · N. Enomoto
First Department of Internal Medicine, University of Yamanashi, Chuo 409-3898, Japan

M. Nakagawa · N. Sakamoto
Department of Gastroenterology and Hepatology, Tokyo Medical and Dental University, Tokyo 113-0034, Japan

N. Sakamoto · S. Hige
Department of Internal Medicine, Hokkaido University Graduate School of Medicine, Sapporo 060-0814, Japan

H. Yatsuhashi
Clinical Research Center, National Nagasaki Medical Center, Omura 856-8562, Japan

M. Kurosaki · N. Izumi
Division of Gastroenterology and Hepatology, Musashino Red Cross Hospital, Musashino 180-0023, Japan

testing for this variant might be useful for establishing personalized drug dosing in order to minimize drug-induced adverse events.

Introduction

Chronic hepatitis C virus (HCV) infection is a significant risk factor for progressive liver fibrosis and hepatocellular carcinoma. Antiviral treatment improves the natural course in chronic hepatitis C (CHC) (George et al. 2009; Yoshida et al. 2004). Newly-developed treatments involving direct-acting antivirals (DAAs), including nonstructural (NS) 3/4A protease inhibitors have shown promising outcomes in combination with pegylated interferon (PEG-IFN) plus ribavirin (RBV) in several clinical trials. Thus, >70 % of patients infected with HCV genotype 1 are reported to achieve sustained virological responses (SVR) (Jacobson et al. 2011; Poordad et al. 2012; Zeuzem et al. 2011). Furthermore, interferon-free (IFN-free) therapies are expected to be useful especially in IFN-resistant patients and may become the standard of care in the near future. However, IFN-based regimens have been standard-of-care therapies over the last couple of decades.

IFN-based therapies are associated with various adverse effects. Cytopenia is common due to bone marrow suppression cased by IFN or DAA and hemolysis by RBV. This is particularly the case in patients with advanced hepatic fibrosis, but can sometimes also occur in those with mild fibrosis. This then often necessitates dose reduction or premature withdrawal from therapy, resulting in poor response to treatment. For instance, it was reported that rates of viral clearance were significantly reduced in patients who could not be maintained on at least 80 % of their drug doses for the duration of PEG-IFN/RBV therapy (McHutchison et al. 2002). Therefore, pre-treatment prediction of possible adverse effects in order to avoid them and undergo therapy safely is desirable.

Recent genome-wide association studies (GWASs) have identified two important host genetic variants influencing CHC treatment: (1) single nucleotide polymorphisms (SNPs) near the interleukin-28B (*IL28B*) gene, which are strongly associated with response to therapy for chronic HCV genotype 1 infection (Ge et al. 2009; Suppiah et al. 2009; Tanaka et al. 2009), and (2) SNPs in the inosine triphosphatase (*ITPA*) gene, which accurately predict RBV-induced anemia in European–American (Fellay et al. 2010) and Japanese population (Ochi et al. 2010). We validated the association between this *ITPA* genetic variant and RBV-induced anemia (Sakamoto et al. 2010), and reported that the *ITPA* genotype affects the tolerated doses of RBV and treatment response in a stratified group (Kurosaki et al. 2011; Matsuura et al. 2014). Additionally, our GWAS showed that *DDRGK1/ITPA* variants are strongly associated with IFN-induced thrombocytopenia as well as anemia during PEG-IFN/RBV therapy (Tanaka et al. 2011). Thompson et al. (2012) also reported that the *ITPA* genetic variant was associated with anemia and thrombocytopenia during PEG-IFN/RBV therapy. However they identified no genetic determinants of IFN-induced neutropenia at the level of genome-wide significance by their GWAS in populations of European Americans, African Americans and Hispanics.

Hence, to identify genetic variants associated with IFN-induced neutropenia, we conducted a GWAS in Japanese CHC patients.

Y. Hiasa
Department of Gastroenterology and Metabology, Ehime University Graduate School of Medicine, Toon 791-0295, Japan

T. Ide
Division of Gastroenterology, Department of Medicine, Kurume University, Kurume 830-0011, Japan

K. Hino
Department of Hepatology and Pancreatology, Kawasaki Medical School, Kurashiki 701-0114, Japan

A. Tamori
Department of Hepatology, Osaka City Graduate School of Medicine, Osaka 545-8585, Japan

M. Honda · S. Kaneko
Department of Gastroenterology, Kanazawa University Graduate School of Medicine, Kanazawa 920-0934, Japan

S. Mochida
Division of Gastroenterology and Hepatology, Internal Medicine, Saitama Medical University, Iruma 350-0495, Japan

H. Nomura
The Center for Liver Disease, Shin-Kokura Hospital, Kitakyushu 803-8505, Japan

S. Nishiguchi
Department of Internal Medicine, Hyogo College of Medicine, Nishinomiya 663-8131, Japan

C. Okuse
Department of Gastroenterology and Hepatology, St. Marianna University School of Medicine, Kawasaki 216-8511, Japan

Y. Itoh
Molecular Gastroenterology and Hepatology, Kyoto Prefectural University of Medicine, Kyoto 602-0841, Japan

H. Yoshiji
Third Department of Internal Medicine, Nara Medical University, Kashihara 634-8522, Japan

I. Sakaida
Department of Gastroenterology and Hepatology, Yamaguchi University Graduate School of Medicine, Ube 755-8505, Japan

Materials and methods

Patients

From 2007 to 2012, samples for the GWAS were obtained from 416 CHC patients who were treated at 22 hospitals (liver units with hepatologists) throughout Japan. In the following stage of replication analysis, samples were collected in an independent set of 404 Japanese CHC patients. Most patients were treated with PEG-IFN-α2b (1.5 μg/kg body weight subcutaneously once a week) or PEG-IFN-α2a (180 μg once a week) plus RBV (600–1,000 mg daily according to body weight) for 48 weeks for HCV genotype 1 and 24 weeks for genotype 2. Treatment duration was extended in some patients up to 72 weeks for genotype 1 and 48 weeks for genotype 2 according to physicians' preferences. Other patients were treated with PEG-IFN-α2a or IFN monotherapy, or IFN-α2b plus RBV in standard doses of the regimens. The doses of drugs were reduced according to the recommendations on the package inserts or the clinical conditions of the individual patients. Erythropoietin or other growth factors were not given. Patients chronically infected with hepatitis B virus or human immunodeficiency virus, or with other causes of liver disease such as autoimmune hepatitis and primary biliary cirrhosis, were excluded from this study. Written informed consent was obtained from all individual participants in this study and the study protocol conformed to the ethics guidelines of the Declaration of Helsinki and was approved by the institutional ethics review committees.

Inclusion criteria of neutropenia

In the initial stage of GWAS, we defined the inclusion criteria of the case group as minimum neutrophil counts of $<750/mm^3$ at week 2 or 4 during IFN-based therapy, since the dose reduction of IFN is recommended at those levels on the package inserts. Thereafter we did it as minimum neutrophil counts of $<600/mm^3$ at week 2 or 4 in the following GWAS and the replication stages.

SNP genotyping and data cleaning

We conducted two stages of GWAS using the Affymetrix Genome-Wide Human SNP Array 6.0 (Affymetrix, Inc. Santa Clara, CA) according to the manufacturer's instructions. The cut-off value was calculated to maximize the difference, which was also close to median change. At GWAS, the average overall call rate of patients in the case and the control group reached 98.66 and 98.79 %, respectively. We then applied the following thresholds for SNP quality control (QC) in data cleaning: SNP call rate ≥95 % for all samples, minor allele frequency (MAF) ≥1 % for all samples. A total of 601,578 SNPs on autosomal chromosomes passed the QC filters and were used for association analysis. All cluster plots of SNPs showing $P < 0.0001$ in association analyses by comparing allele frequencies in both groups were checked by visual inspection and SNPs with ambiguous genotype calls were excluded. In the replication study, the genotyping of 192 candidate SNPs in an independent set of 404 Japanese HCV-infected patients was carried out using the DigiTag2 assay (Nishida et al. 2007). Successfully genotyped SNPs in the replication analysis had a >95 % call rate, and cleared Hardy–Weinberg equilibrium (HWE) $P \geq 0.001$. One SNP could not be genotyped, and hence we obtained data on 191 SNPs including rs9915252. Three SNPs, rs4794822, rs3907022, and rs3859192 located around the proteasome 26S subunits non-ATPase 3 (*PSMD3*) gene and rs8099917 near the *IL28B* gene were genotyped by TaqMan SNP Genotyping Assays (Applied Biosystems, Carlsbad, CA) following the manufacturer's protocol.

Laboratory and histological tests

Blood samples were obtained at baseline and at appropriate periods after the start of therapy and for hematologic tests, blood chemistry, and HCV RNA. Fibrosis was evaluated on a scale of 0–4 according to the METAVIR scoring system. The SVR was defined as an undetectable HCV RNA level by Roche COBAS Amplicor HCV Monitor test, v.2.0 (Roche Molecular Diagnostics, Pleasanton, CA) with a lower detection limit of 50 IU/ml or Roche COBAS AmpliPrep/COBAS TaqMan HCV assay (Roche Molecular Diagnostics, Pleasanton, CA) with a lower detection limit of 15 IU/ml 24 weeks after the completion of therapy. Serum granulocyte colony-stimulating factor (G-CSF) levels were analyzed using Human G-CSF Quantikine ELISA Kit (R&D Systems, Inc., Minneapolis, MN).

K. Yamamoto
Department of Gastroenterology and Hepatology, Okayama University Graduate School of Medicine, Dentistry, and Pharmaceutical Sciences, Okayama 700-0914, Japan

H. Watanabe
Department of Gastroenterology, Yamagata University Faculty of Medicine, Yamagata 990-9585, Japan

S. Hige
Department of Gastroenterology, Sapporo Kosei General Hospital, Sapporo 060-0033, Japan

A. Matsumoto · E. Tanaka
Department of Medicine, Shinshu University School of Medicine, Matsumoto 390-8621, Japan

Expression quantitative trait locus analysis

Expression quantitative trait locus analysis (eQTL) was conducted using the web-based tool, Genevar (http://www.sanger.ac.uk/resources/software/genevar) (Yang et al. 2010). We evaluated the correlations between rs2305482 genotypes and the expression of transcripts of *PSMD3* or colony-stimulating factor 3 (*CSF3*) by the Spearman's rank correlation coefficient.

Statistical analysis

In the GWAS and the replication stages, the observed association between a SNP and neutropenia induced by IFN-based therapy was assessed by the Chi square test with a two-by-two contingency table in three genetic models: the allele frequency model, the dominant-effect model and the recessive-effect model. Significance levels after Bonferroni correction for multiple testing were $P = 8.31 \times 10^{-8}$ (0.05/601,578) in the GWAS stage and $P = 2.62 \times 10^{-4}$ (0.05/191) in the replication stage. Categorical variables were compared between groups by the Chi square test, and non-categorical variables by the Student's *t* test or the Mann–Whitney *U* test. Multivariate logistic regression analysis with stepwise forward selection was performed with $P < 0.05$ in univariate analysis as the criteria for model inclusion. To evaluate the discriminatory ability of neutrophil counts at baseline to predict neutropenia during IFN-based therapy, receiver operating characteristic curve (ROC) curve analysis was conducted. Changes of serum G-CSF levels from baseline to the period with neutropenia during IFN-based therapy were compared by the repeated measure analysis of variance (ANOVA). Correlations between neutrophil counts and serum G-CSF levels were analyzed using Pearson's correlation coefficient test. $P < 0.05$ was considered significant in all tests.

Results

Genetic variants associated with IFN-induced neutropenia

We conducted two stages of GWAS by changing the terms of neutrophil counts, followed by the replication analysis (Fig. 1). The characteristics of the patients in each group for the GWAS and the replication stage are summarized in Table 1. At the first stage of GWAS (GWAS-1st), we genotyped 416 Japanese CHC patients with minimum neutrophil counts of <750/mm^3 (Case-G1, $n = 114$) and ≥1,000/mm^3 (Control-G, $n = 302$) at week 2 or 4 during IFN-based therapy. Here there may still be mixed with undesirable samples that should be removed from the case group. Therefore, we designed and carried out the second stage of GWAS (GWAS-2nd) comparing the patients with more severe neutropenia to the control group: in patients with minimum neutrophil counts of <600/mm^3 (Case-G2, $n = 50$) and ≥1,000/mm^3 (Control-G, $n = 302$) at week 2 or 4 using the same samples as used in GWAS-1st. Supplementary Fig. 1 shows a genome-wide view of the single-point association data based on allele frequencies in GWAS-1st and GWAS-2nd. No association between SNPs and IFN-induced neutropenia reached a genome-wide level of significance [Bonferroni criterion $P < 8.31 \times 10^{-8}$ (0.05/601,578)]. Therefore, we selected the candidate SNPs principally

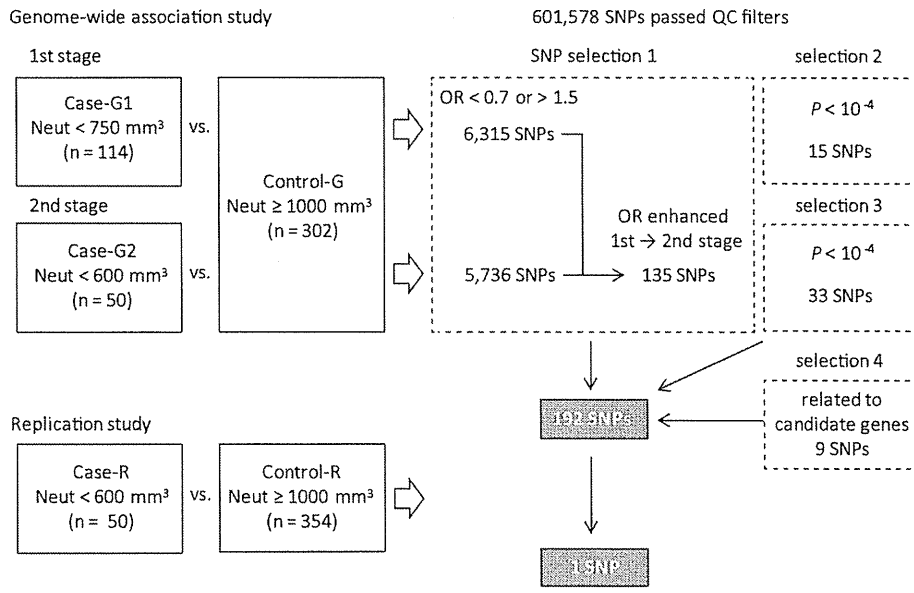

Fig. 1 Outline of the study design. *Neut* neutrophil counts, *SNP* single nucleotide polymorphism, *QC* quality control, *OR* odds ratio

Table 1 Clinical characteristics of patients in GWAS and the replication study

	GWAS			Replication study	
	Case-G1 ($n = 114$)	Case-G2 ($n = 50$)	Control-G ($n = 302$)	Case-R ($n = 50$)	Control-R ($n = 354$)
At baseline					
Gender, male/female	48/66	21/29	170/132	24/26	208/146
Age, years	57.9 (8.7)	57.1 (8.3)	57.2 (11.2)	59.1 (10.2)	56.7 (9.6)
Neutrophil count, /mm^3	1,800 (777)	1,662 (897)	2,750 (984)	1,570 (552)	2,724 (985)
Hemoglobin, g/dL	13.6 (1.3)	13.5 (1.3)	14.2 (1.5)	13.6 (1.6)	14.3 (1.5)
Platelet count, $\times 10^9$/L	141 (42)	132 (46)	164 (54)	140 (47)	162 (60)
ALT, IU/L	82.9 (88.6)	70.4 (53.1)	81.5 (77.9)	87.8 (82.7)	85.2 (71.1)
HCV genotype, 1/2/ND	95/18/1	40/10/0	250/51/1	45/5/0	277/77/0
HCV RNA, log IU/mL	5.9 (0.8)	5.9 (1.0)	6.1 (0.8)	6.1 (0.9)	6.1 (0.8)
Liver fibrosis, F0-2/F3-4/ND	62/22/30	25/10/15	168/70/64	21/6/23	229/87/38
rs8099917, TT/TG + GG/ND	74/39/1	35/15/0	189/109/4	31/17/2	278/70/6
Regimen					
PEG-IFN + RBV/IFN + RBV/PEG-IFN/IFN mono	112/0/0/2	48/0/0/2	277/9/9/7	44/4/2/0	351/0/3/0
At week 4					
Neutrophil count, /mm^3	606 (126)	496 (104)	1,551 (501)	501 (89)	1,533 (484)

Data are expressed as number for categorical data or the mean (standard deviation) for non-categorical data

GWAS genome-wide association study, *ALT* alanine transaminase, *ND* not determined, *PEG-IFN* pegylated interferon, *IFN* mono, interferon monotherapy, *RBV* ribavirin

by comparing between GWAS-1st and GWAS-2nd as follows. There were 6,315 and 5,736 SNPs with odds ratios (ORs) <0.7 or >1.5 at GWAS-1st and GWAS-2nd, respectively. Of these, the ORs of 135 SNPs were more notable at GWAS-2nd than at GWAS-1st. In addition to the 135 SNPs, we selected 15 and 33 SNPs with $P < 10^{-4}$ at GWAS-1st and GWAS-2nd, and added 9 SNPs which are located around the candidate genetic regions identified by the GWAS stage and are non-synonymous or related to diseases in previous reports. Consequently, we carried out the replication analysis focusing on this total of 192 SNPs.

In the subsequent replication analysis, we carried out genotyping of the 192 candidate SNPs in an independent set of 404 Japanese HCV-infected patients with minimum neutrophil counts of <600/mm^3 (Case-R, $n = 50$) and ≥1,000/mm^3 (Control-R, $n = 354$) at week 2 or 4 during IFN-based therapy (Table 1; Fig. 1). The results in the replication stage combined with GWAS-2nd are shown in Supplementary Table 1. Several SNPs such as rs11743919 and rs2457840 showed strong associations with low P value, however, the MAF of them were <5 %. In general, low frequent SNPs tend to show unsettled associations, especially in statistical analysis with small number of samples. Therefore, we excluded these SNPs from the final candidates. Consequently, we determined the SNP rs2305482, located in the intron of *PSMD3* gene on chromosome 17, as the most promising candidate, which showed a strong association with IFN-induced neutropenia in the combined results of GWAS-2nd and the replication stage (OR = 2.18; 95 % CI = 1.61–2.96, $P = 3.05 \times 10^{-7}$ in the allele frequency model) (Table 2).

Association of SNPs located in *PSMD3-CSF3* with neutropenia

A previous GWAS showed that rs4794822 located between the *PSMD3* and *CSF3* genes was associated with neutrophil counts in Japanese patients including 14 different disease groups (Okada et al. 2010). As shown in Fig. 2, rs4794822 is in strong linkage disequilibrium (LD) with rs2305482 which we identified in the present study. Thus, the pairwise LD (r^2) in the HapMap JPT: Japanese in Tokyo, Japan, is 0.66. Because the SNP rs4794822 is not included in the Affymetrix Genome-Wide Human SNP Array 6.0, we additionally genotyped it together with three other SNPs (rs9915252, rs3859192 and rs3907022) located in the same LD block around the *PSMD3* gene (Fig. 2). The allele frequency of each SNP was compared between patients with minimum neutrophil counts of <600/mm^3 (Case-G2 + R: Case-G2 plus Case-R, $n = 100$) and ≥1,000/mm^3 (Control-G + R: Control-G plus Control-R, $n = 656$) at week 2 or 4 during IFN-based therapy. This showed that, rs4794822 was also strongly associated with neutropenia during IFN-based therapy (OR = 2.24; 95 % CI = 1.63–3.07, $P = 3.63 \times 10^{-7}$ in the allele frequency model) (Table 3).